Journal of Chemical&Engineering Data

pubs.acs.org/jced
Review

Deep Eutectic Solvents Meet Non-Aqueous Cosolvents: A Modeling and Simulation Perspective—A Tutorial Review

Leon de Villiers Engelbrecht,[#] Narcis Cibotariu,[#] Xiaoyan Ji,[*] Aatto Laaksonen,[*] and Francesca Mocci[*]

Cite This: *J. Chem. Eng. Data* 2025, 70, 19−43

ABSTRACT: Deep eutectic solvents (DESs) have recently gained attention due to their tailorable properties and versatile applications in several fields, including green chemistry, pharmaceuticals, and energy storage. Their tunable properties can be enhanced by mixing DESs with cosolvents such as ethanol, acetonitrile, and water. DESs are structurally complex, and molecular modeling techniques, including quantum mechanical calculations and molecular dynamics simulations, play a crucial role in understanding their intricate behavior when mixed with cosolvents. While the most studied cosolvent is water, in some applications, even a small content of water is considered a contaminant, for example, when the processes of interest require dry conditions. Only quite recently have modeling studies begun to focus on DES mixed with cosolvents other than water. This tutorial provides the first comprehensive overview of these studies. It highlights how modern molecular modeling increases our understanding of their structural organization, transport properties, phase behavior, and thermodynamic properties. Additionally, case studies and recent developments in the field are discussed along with the challenges and future directions in molecular modeling of DES in cosolvent mixtures. Overall, this review offers valuable insights into the molecular-level understanding of DES-cosolvent systems and their implications for designing novel solvent mixtures with tailored properties for various applications.

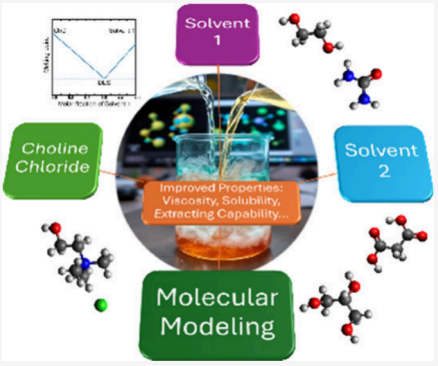

1. INTRODUCTION

In the growing field of green chemistry, an essential step is to minimize the environmental effects of the solvents and to enhance their safe use. This has put the focus on ionic liquids (ILs) and, more recently, on deep eutectic solvents (DESs), that consist entirely or in part of ions.[1] A key advantage of ILs and DESs over traditional organic solvents is their much lower, often negligible, vapor pressure under ambient conditions, resulting in lower human health risk. Furthermore, they are often characterized by high thermal stability and are less flammable than other electrolytes.[2] Today, ILs and DESs are not only green solvents but also found in numerous applications in a wide variety of areas for their unique properties and tunability as tailorable substances. Here we will focus entirely on DES with cosolvents other than water.

The term DES refers to the eutectic mixtures of a hydrogen bond acceptor (HBA) and a hydrogen bond donor (HBD) for which the eutectic point is very low, compared to that of the individual components, as originally observed for reline, a mixture of choline chloride (ChCl) and urea at the eutectic composition of a 1:2 molar ratio.[3] However, under the category of DES, many mixtures with interesting properties are often (incorrectly) classified, even when their compositions do not lie at the eutectic point or involve compounds that can form a eutectic mixture rather than a true deep eutectic mixture.[4−6] In a recent study, a computational procedure was developed, supported by experimental data, to enable a priori predictions of DES formation.[7] A common feature of DESs is that the formation of HBA-HBD hydrogen bonds (H-bonds) disrupts the crystal structures of the individual components, resulting in a melting point lower than that of either component. This process enables the use of DESs as a liquid medium for chemical reactions, offering a solvent environment that is both versatile and eco-friendly.

DESs are typically classified into five types (I−V), primarily on the basis of the nature of the HBA and HBD that compose them. Types I−III are composed of a quaternary ammonium salt plus a metal chloride (Type I), or a metal chloride hydrate (Type II), or an organic molecular component, such as an amide, carboxylic acid, or polyol (Type III). In the latter DES type, the quaternary ammonium salt acting as HBA is typically ChCl.[8] Differently from Types I−III, in Type IV, HBA is a metal hydrate. Type V substantially differs from the other types of DES, with both HBA and HBD being nonionic molecular

Received: September 7, 2024
Revised: October 17, 2024
Accepted: October 31, 2024
Published: December 6, 2024

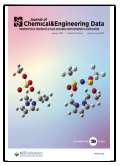

https://doi.org/10.1021/acs.jced.4c00505
J. Chem. Eng. Data 2025, 70, 19−43

compounds.[9] The diversity of DES types allows for precise tuning to specific tasks, making them highly versatile across various applications. This adaptability extends from organic synthesis and electrochemistry to pharmaceutical formulation and materials science. The Type III DESs, specifically those based on ChCl, have attracted considerable research interest during the past two decades and are by far the most studied DES class.[1,10] The high popularity of this type of DES is mainly due to its easy preparation from inexpensive components and its environmental compatibility and safety.

The properties of DESs can also be altered by adding a third component to the mixture. In general, there are three main motivations for studying and developing DES + cosolvent mixtures: i) Solvents are added intentionally to DES to modify their properties, e.g., to reduce viscosity, improve electrical conductivity (electrochemical applications), change the polarity or other solvent properties (e.g., H-bonding characteristics), notably in studies involving proteins or other biological macromolecules like lignin. ii) Third components can be inadvertently introduced, e.g., due to DES hygroscopicity or other impurities, or they may enter the DES specifically due to the field of application, e.g., when DESs are used as liquid−liquid extraction media. iii) This could be considered a special case of i), when limited specific amounts of a third component or solvent (e.g., water) may be added to a DES in order to produce a new ternary DES (TDES) with improved or otherwise desirable properties, e.g., further reducing the viscosity or melting point.

The most studied third component to DES mixtures is water, and it is commonly known that it can strongly affect the DES properties even when added in very small amounts.[11] DES mixtures with nonaqueous third components (NATCs) are important in many cases, such as those in which the water presence can alter the kinetics of a chemical or physical process that should occur in DES-based solvent, or when the reagent or byproduct is insoluble, immiscible, or unstable in water. Water is also undesirable in some industrial applications, e.g., in the fuel industry. Despite the fact that the study of DES mixtures with NATCs is still much more limited compared to that of DES + water systems, the modeling of these systems is rapidly emerging as a fundamental tool to predict and understand their properties. The structural organization and/or the structural and dynamical properties of DES + cosolvent complex systems molecularly are due to the multitude of intermolecular interactions. These strong, long-living interactions create distinct, far-reaching liquid structures. Their structure can be experimentally studied using a variety of spectroscopic techniques, from NMR and IR to MS and scattering experiments. The structures of DES and IL systems with cosolvents can be highly intricate, making molecular modeling critically important for resolving heterogeneities, long-range structuring, and viscosity issues and for obtaining a detailed molecular picture of the interactions. The following studies provide further insight.[11−16] Recent reviews, concerning the modeling of mixtures of DES with cosolvents, have been focusing mainly on water as cosolvent,[17,18] while, to the best of our knowledge, no review has been so far dedicated to the more challenging modeling of DES + NATC, despite the increasing amount of experimental investigations reported in the literature.[19−21]

The most studied NATCs are alcohols since they also reduce viscosity and are of interest in fuel-related extraction applications. Also, aprotic polar solvents like dimethyl sulfoxide (DMSO), acetonitrile (ACN), etc. reduce viscosity and polarity and modify H-bonding characteristics. In addition, a variety of NATCs have been studied so far. Figure 1 and Table 1 summarize the DES + NATC systems that, to the best of our knowledge, have been modeled by molecular dynamics (MD), Monte Carlo (MC), and quantum mechanical (QM) calculations for Type III, ChCl-based DESs.

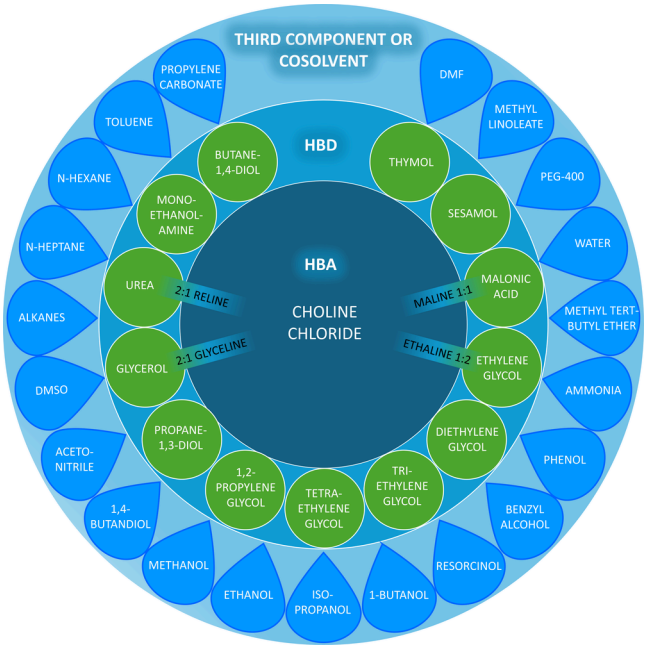

Figure 1. Schematic representation of the components of ChCl-based DES systems modeled in the presence of at least one additional component. The HBD of the DES is represented by a green circle, while cosolvents are depicted as azure drops. Some DESs have specific names, which are shown within rectangular shapes connecting the HBD with the HBA, along with the corresponding molar fractions. Further details on the specific combinations of DES components and cosolvents are provided in Table 1, along with the corresponding reference.

Reading the still limited number of published studies so far already indicates that molecular modeling is critically valuable in understanding the molecular-level effects of cosolvents or impurities on the physicochemical properties of DESs. And, not at least, water (or organic solvents) can often be found in trace amounts in them as impurities due to the hygroscopic nature of DESs. In the following, we briefly describe different models and modeling techniques that have been used and the properties that can be calculated using these techniques (Section 2). We then illustrate various applications by describing the selected studies conducted on type III DES + NATC up until May 2024 in Section 3. Note that computational studies of DES + water have been reviewed, e.g., by Kaur et al.[17] and Tomalchev et al.,[18] and are not included here. Concluding remarks are finally given in Section 4.

2. COMPUTATIONAL METHODS

The two categories of modeling techniques that have been used to model the DES + third component systems at the molecular level are i) the classical force field-based MD simulations,[44−46] and ii) quantum chemistry (QC) methods, density functional theory (DFT) and COnductor-like Screen-

https://doi.org/10.1021/acs.jced.4c00505
J. Chem. Eng. Data 2025, 70, 19−43

Table 1. Composition of Systems Comprising DES and Third Components Studied by Molecular Modeling[a]

HBA	HBD	Cosolvent/ 3rd component	MD/MC simulations	QM calculations
Reline and reline related				
ChCl	urea (1:2)	1-butanol	22	
ChCl	urea (1:2)	*n*-hexane	23	
ChCl	urea (1:2)	*n*-heptane	22, 24	
ChCl	urea (1:2)	MeOH	23, 25−27	25
ChCl	urea (1:2)	MTBE	25	25
ChCl	urea (1:2)	PC	27	
ChCl	urea (1:2)	IPA	24	28
ChCl	urea (1:2)	DMSO	29, 30	30
ChCl	urea (1:2)	PEG400	31	31
ChCl	urea (1:2)	EtOH	26	
ChCl	urea (1:2)	resorcinol, water	32	
ChCl	urea (1:2)	resorcinol, BA	33	
Ethaline, glyceline, and other mixtures of ChCl with glycols and alcohols				
ChCl	EG (1:2)	1-butanol	22	
ChCl	EG (1:2)	MeOH	23, 25, 27, 34, 35	25
ChCl	EG (1:2)	PC	27	
ChCl	EG (1:2)	MTBE	25	25
ChCl	EG (1:2)	IPA	24	28
ChCl	EG (1:2)	DMSO	30	30
ChCl	EG (1:2)	PEG400	31	31
ChCl	EG (1:2)	ACN		36
ChCl	EG (1:2)	DMF		37
ChCl	EG (1:2)	*n*-hexane	23	
ChCl	EG (1:2)	*n*-heptane	22, 24	
ChCl	EG (1:2)	phenol, toluene	38	38
ChCl	DEG (1:2.5)	phenol, toluene	38	38
ChCl	TEG (1:3)	phenol, toluene	38	38
ChCl	TTEG (1:3.5)	phenol, toluene	38	38
ChCl	EG (1:4)	*n*-heptane	39	39
ChCl	DEG (1:1), DEG (1:2), DEG (1:4)	*n*-heptane	39	39
ChCl	1,3PDO (1:2)	MeOH, MTBE	25	25
ChCl	PG (1:2)	1-butanol, *n*-heptane	22	
Ethaline, glyceline, and other mixtures of ChCl with glycols and alcohols				
ChCl	1,4BDO (1:2)	MeOH, MTBE	25	25
ChCl	sesamol (1:3)	MeOH	40	
ChCl	thymol (1:7)	*n*-hexane	41	
ChCl	GC (1:2)	1-butanol	22	
ChCl	GC (1:2)	MeOH	23, 25, 34	25
ChCl	GC (1:2)	MTBE	25	25
ChCl	GC (1:2)	*n*-hexane	23	
ChCl	GC (1:2)	*n*-heptane	22, 24	
ChCl	GC (1:2)	IPA	24	
ChCl	GC (1:2)	DMSO	30	
ChCl	GC (1:2)	PEG400	31	31
ChCl	GC (1:5)	resorcinol, NH_3	42	
ChCl	MEA (1:4)	*n*-heptane	39	39
Maline and other mixtures of ChCl with carboxylic acids				
ChCl	MA (1:1)	MeOH, MTBE	25	25
ChCl	MA (1:2)	IPA		28
Mixtures of HBA other than ChCl with glycols				
TBAC	EG (1:3)	MeOH, ACN	43	43
TBAB	DEG (1:4)	*n*-heptane	39	39
TBAP	DEG (1:4)	*n*-heptane	39	39

[a]The table includes the nature of the HBA, HBD with their molar ratios, cosolvents, or third components, and references divided into MD or MC simulations and QC calculations. Systems are grouped into four categories: reline and related; ethaline, glyceline, and ChCl with glycols/alcohols; maline and ChCl with carboxylic acids; and mixtures of HBAs other than ChCl with glycols. Abbreviations used for the compounds: ethylene glycol (EG), diethylene glycol (DEG), triethylene glycol (TEG), tetraethylene glycol (TTEG), glycerol (GC), malonic acid (MA), propylene glycol (PG), polyethylene glycol 400 (PEG400), methanol (MeOH), ethanol (EtOH), isopropanol (IPA), propane-1,3-diol (1,3PDO), butane-1,4-diol (1,4BDO), benzyl alcohol (BA), propylene carbonate (PC), methyl linoleate (ML), methyl tert-butyl ether (MTBE), monoethanolamine (MEA), acetonitrile (ACN), dimethylformamide (DMF), tetrabutylphosphonium bromide (TBAP), tetrabutylammonium bromide (TBAB), tetrabutylammonium chloride (TBAC).

ing MOdel for Realistic Solvation (COSMO-RS).[47] We will also suggest additional methods and techniques to tackle the high complexity of the DES systems. These two types of methods are complementary in describing such complex liquid mixtures where aspects, such as electronic polarization and solvation thermodynamics, are important. Not surprisingly, the COSMO-RS is an ideal tool here.

Additionally, statistical associating fluid theory (SAFT) is a modeling method used in molecular thermodynamics to predict the phase behavior of complex fluids.[48] In particular, SAFT is a molecular-based equation of state that describes the Helmholtz free energy in closed algebraic form and is formulated explicitly in terms of a predefined intermolecular potential, which makes it feasible to combine with the advanced models (computer simulation models) with transferable parameters.

In SAFT, molecules are described as chains of spherical segments with interactions (dispersion, repulsion, H-bonds, etc.) and it is particularly useful for predicting the properties of mixtures and nonideal fluids. SAFT and its many extensions and improvements, including perturbed-chain SAFT (PC-SAFT), have been extensively used for IL systems, but its application on DESs is very limited. We wish to promote this method as both simple and powerful, especially with the latest extensions (see references 49−55), and suggest it as a valuable complement to COSMO-type schemes in capturing the complexities of DES systems.

2.1. Molecular Dynamics Simulations. The MD technique is a well-established computer simulation technique where the temporal evolution of the position of atoms and molecules over time is calculated for a model system containing often from tens to even hundreds of thousands of atoms. No better modeling method currently exists for investigations of the structural, thermodynamic, and dynamical properties of complex liquid mixtures such as ILs, not to mention the more complicated DES and their mixtures with

https://doi.org/10.1021/acs.jced.4c00505
J. Chem. Eng. Data 2025, 70, 19−43

cosolvents. In MD simulations, the model system is built in a small simulation cell with translational symmetry (periodicity) and specific coordinates for all atoms in molecules. Periodic boundary conditions (PBC) and minimum image conventions are used to maintain the number of atoms in the cell and their uniform distribution. The atoms get both their velocities and accelerations when the simulation is started after numerically solving Newton's equations of motion for all particles with masses. The force (in $F_i = m_i a_i$), directed to act on each individual atom, coming from all interactions with all surrounding atoms, is taken as the negative spatial derivative of the used force field (FF). In MD simulations, Newton's equations are solved repeatedly after short time increments called time steps (typically 1−2 fs), and this is done until long enough simulation times are covered, typically from hundreds of nanoseconds to milliseconds.[44,46] In practice, the accelerations of atoms are first integrated to obtain their velocities, and the velocities are integrated thereafter to obtain the new positions. The digitized movements (coordinates, velocities, etc.) of the molecular systems can be saved as trajectories on a hard disk and analyzed and visualized at any moment of convenience. Various properties can be calculated by using statistical thermodynamics tools and compared with experiments if available. Physical conditions in the simulation cell can be fixed by using thermostats and/or barostats. Various enhanced techniques can be used to improve the sampling. MD simulations are crucial, for example, in understanding how the addition of a cosolvent affects the structural, dynamic, and thermodynamic properties of the DES. MD simulations provide insights into solvation dynamics, miscibility, and the potential enhancement or inhibition of certain properties, aiding in the design and optimization of DESs for various applications in fields such as chemistry, biophysics, and materials science. The accuracy of these simulations depends on the quality of the potential energy functions used in the force fields, modeling the interatomic forces within the DES-cosolvent system.

2.1.1. Force Fields and Parameters for DES and Cosolvents. The quality of the force field in all-atom computer simulations is of tantamount importance. In the case of DES and IL systems, the choices of the force field can be particularly slim for several reasons. ILs and DESs, as a heterogeneous composition of cations and anions, acceptors, and donors of H-bonds, etc., show a broad spectrum of interactions not only with themselves but also with other molecular systems, including cosolvents, in their vicinity. It is challenging to describe them well due to their high complexity and to find a balance in a composition of short-ranged van der Waals and long-range electrostatic, ionic, HB, and $\pi-\pi$ stacking. In addition, IL systems are easily polarizable and show even charge transfer in their aromatic ring moieties, which is not commonly considered in the development of standard types of force fields. As molecular salts, they can be both bulky and flexible, with large amplitude conformational changes in their long tails, thereby needing proper intramolecular degrees of freedom. Internal structure and dynamics should be well described by the force fields, as they have a big effect on the viscosity by entangling around each other. As highly charged systems, they exhibit strong screening effects. Their properties and behavior, in general, are far from those of ideal or more inert systems. Besides, there are almost an astronomical number of possible IL systems (order of 10^{18}) with a great structural and chemical variety, making any force field difficult to be transferred from one system to another. Being nonstandard types of molecules, it is difficult to use parameters from other common force fields and readjust them to ILs. At the same time, and there is still a lack of experimental data to use to fit new parameters in the force fields.[56,57] The development of force fields for ILs is demanding in terms of both time and computer resource demand. For example, we can take the charge transfer mechanism requiring advanced QM methods. Ishizuka and Matsubashi[58] present a laborious iterative self-consistent scheme to obtain "charge-transfer diluted" atomic charges by combining QC and MD simulations. Their results show that a scaling factor 0.8, commonly used by the IL simulation community, is a reasonable approximation.

Currently, many applications of ILs and DESs use them embedded on surfaces, and this makes it difficult to use standard force fields, originally developed for isotropic systems. Large errors can be encountered, as small uncertainties tend to accumulate in anisotropic environments, while in isotropic systems, they can cancel out. It should also be kept in mind that ILs and DESs are more sensitive to temperature and pressure fluctuations than normal liquids, and this cannot be considered in parametrizing conventional force fields.

Many of the problems mentioned above could be corrected by using polarizable force fields and ab initio simulations. These are expensive to use for ILs that have long-range correlations and require long simulations to get properly equilibrated. In the future, we will see accurate coarse-grained force fields for ILs[15,59,60] where electrostatic interactions are included implicitly or explicitly. Very important contribution will come from integrating machine learning in the development of force fields even for DES systems.[61]

As can be seen from Table 2, to date, the force fields mostly used for the modeling of the DES + NATC system are those of the Generalized Amber Force Field (GAFF)[62,63] and their DES-oriented modifications by Perkins et al.,[64,65] those from the OPLS-AA force field developed by Jorgensen group[66−68] and their IL or DES-oriented modifications by Canongia Lopez and Padua[69] as well as by Doherty and Acevedo,[70] and the GROMOS 54A7 force field.[71−73] To the best of our knowledge, a comparison of their performances for DES + NATC mixtures has not been reported and would certainly be welcomed by the growing community interested in their applications.

2.1.2. Simulation Software Packages and Protocols Used. Three simulation packages are used in the studies, which were reviewed here: GROMACS,[74] Amber,[75] and LAMMPS.[76] GROMACS (GROningen MAchine for Chemical Simulations) is an open-source, high-performance MD simulation software, originally optimized for biomolecules, such as proteins, lipids, and nucleic acids. It is very easy to use and is widely popular due to its speed and efficiency. It scales excellently in a variety of parallel architectures from CPU to GPU. It is well-documented with a vast user community. It supports many force fields and types of simulations. Although it is used in most studies, it may not always be flexible enough to handle complex force fields developed for ILs. Also, it may provide a limited support for nonbiomolecular systems. Similarly, Amber (Assisted Model Building and Energy Refinement) is also developed originally for biomolecular systems (proteins and nucleic acids), offering many different force fields while continuously developing their own Amber force fields. It has good facilities to build up systems to

https://doi.org/10.1021/acs.jced.4c00505
J. Chem. Eng. Data 2025, 70, 19−43

Table 2. Force Fields and Software Used in DES + NATC MD/MC Simulations

ChCl	Solvent	NATC	Software	Ref
GAFF	GAFF (urea, EG, GC)	GAFF (DMSO)	GROMACS 4.5.5	30
AMBER[a]	AMBER[a]	AMBER[a]	GROMACS 4.5.4	42
GROMOS 54A7[b]	GROMOS 54A7[b] (urea)	Strader and Feller[b78] (DMSO)	GROMACS 2018.3	29
GAFF	GAFF (urea, EG, GC)	GAFF (PEG400)	GROMACS 5.0	31
GAFF[c]	GAFF[c] (urea)	OPLS-AA (resorcinol)	GROMACS[h]	32
GAFF[c]	GAFF[c] (urea)	OPLS-AA (resorcinol, BA)	GROMACS[h]	33
OPLS[d]	OPLS-AA (sesamol)	OPLS-AA (MeOH)	GROMACS 2020.2	40
GAFF	GAFF (urea, EG, GC, PG)	GAFF (1-butanol, *n*-heptane)	GROMACS[h]	22
GAFF	GAFF (urea, EG, GC)	GAFF (IPA, *n*-heptane)	*h*	24
GAFF	GAFF (urea, EG, GC)	GAFF (MeOH, *n*-hexane)	GROMACS[h]	23
GAFF	GAFF (MA, 1,4BDO, GC, 1,3PDO, urea, EG)	GAFF (MeOH, MTBE)	GROMACS 2019	25
OPLS-AA[e]	OPLS-AA[e] (EG, GC)	OPLS-AA (MeOH)	GROMACS 5.1.4	34
OPLS-AA[e]	OPLS-AA[e] (urea)	OPLS-AA (MeOH, ethanol)	GROMACS 2020.2	26
GAFF[c]	GAFF[c]	GAFF[c]	AMBER 16	35
GAFF[f]	GAFF[f]	OPLS (PC); TraPPE (MeOH, CO_2)	LAMMPS MC: Brick-CFCMC;	27
OPLS-AA	OPLS-AA	OPLS-AA[g]	GROMACS 5.1.4	43
a	*a*	*a*	GROMACS 2019.1	39
OPLS[d]	OPLS-AA (thymol)	OPLS-AA (*n*-hexane)	GROMACS 2020.6	41
GAFF	GAFF (EG, DEG, TEG, TTEG)	GAFF (phenol, toluene)	GROMACS 2020.3	38

[a]No details specified. [b]The authors report the parameters in their Supporting Information. [c]GAFF parameters reported by Perkins.[64] [d]OPLS-compatible parameters developed by Canongia Lopes and Pádua.[69] [e]OPLS-AA force field parameters for ChCl, EG, and GC developed by Doherty and Acevedo.[70] [f]Ionic charges scaled by 0.8 (reline) or 0.9 (ethaline). [g]The parameters were obtained from LigParGen[66] based on OPLS-AA. [h]Software/version not mentioned.

simulate, and it offers advanced techniques for free energy calculations. The current version is free of charge for academic users. LAMMPS (Large-scale Atomic/Molecular Massively Parallel Simulator) is designed for more general and materials science problems, including ILs. It supports a wide range of interaction potentials and is highly extensible. It is useful for complex systems. It scales well on parallel platforms. It requires more setup and experience in scripting and customization but is still the most flexible of the three. These three simulation software are compared in ref 77.

2.2. Quantum Mechanical Modeling Methods. Molecular quantum mechanics contains the electronic degrees of freedom of atoms and molecules and is, therefore, the most fundamental and accurate level used in modeling. Currently, computers are not powerful enough for us to use these first-principles methods without rather severe approximations. Below, we give a short overview of those used in the studies.

2.2.1. Quantum Chemistry Tools. Quantum Chemistry methodologies have developed, matured, and been used in all fields of molecular sciences. They did start from electronic structure and molecular property calculations but are now used as routine tools in materials science and enzymatic catalysis. They can be performed at a variety of theoretical levels from semiempirical to nonempirical Hartree−Fock (HF) and density functional theory (DFT) within mean field approximation. Beyond the so-called post-Hartree−Fock methods, including electron correlation effects, the Møller−Plesset perturbation theory was applied and coupled cluster schemes. DFT is currently the most popular QC method, being computationally as efficient as HF but able to incorporate some of the electron correlations, making it more accurate. QM calculations go into first-principles MD simulations, including Car−Parrinello, and hybrid methods, such as QM/MM. Some software can utilize periodicity, which is important in materials scientific applications.

2.2.2. COSMO. COSMO-RS (Conductor-like Screening Model for Real Solvents) was presented by Klamt in the mid-90s as a computational method to predict the thermodynamic properties of liquid-phase chemical systems.[47] It quickly gained popularity, as it could provide accurate predictions of solubility, vapor−liquid equilibria, and partition coefficients without experimental data.

The use of the COSMO-RS method starts with QM calculations, for example, DFT, to obtain the electronic structure of a molecule. The molecule is then placed in a conductor environment, which produces an electrostatic potential. The surface is divided into small segments with a separate charge density, providing polarity on the entire molecular surface. All of this is the COSMO phase of the calculations.

After that, statistical thermodynamics is applied, where the charge densities are used to calculate interaction energies between the divided segments and between segments and the surrounding solvent. The interaction energies can be used to calculate several thermodynamic properties connected to the solubility of the molecular system from the COSMO phase in the Real Solvent (RS) phase. COSMO-RS is popular, particularly in chemical engineering, due to its accurate predictions of several thermodynamic properties in complex liquid mixtures without empirical data; therefore, no fitting is needed. Also, it is flexible and can be applied to a wide variety of systems, from nonideal electrolytes to organic solvents, biomolecular pharmaceutical systems, and in particular cases where experimental data is limited.[79] It is computationally efficient as a QM method, as calculations are done on individual molecules, and it can be easily combined with other modeling tools and integrated into databases.

The COSMO-SAC (Conductor-like Screening Model-Segment Activity Coefficient) method by Lin and Sandler[80] is a

https://doi.org/10.1021/acs.jced.4c00505
J. Chem. Eng. Data 2025, 70, 19−43

similar computational scheme to COSMO-RS, but it is an empirical approach to the segment interactions, while COSMO-RS is more rigorous based on statistical mechanics. Also, COSMO-SAC can be used to calculate activity coefficients and predict phase equilibria. It is simpler and faster with a more approximate treatment of interactions.

When DESs and ILs are used to meet various extraction issues, the COSMO model proves to be useful in improving the efficiency of chemical extraction operations. σ-profile analysis is used to highlight how the model affects extraction efficiency optimization.

2.3. Solvation Properties. This section is devoted to the properties that can be calculated from molecular simulations and compared to experimental observables.

2.3.1. Molar Fraction. As is the case for computer simulation studies of other liquid mixtures, DES + cosolvent mixture compositions are usually expressed as a molar ratio or mole fraction. Different mole fraction definitions for Type III DES + cosolvent systems are reported in the literature,[26,81] and it is often simply a case of converting from one convention to the other to ensure consistency with experiment. The choice of mole fraction definition becomes crucially important when calculating certain properties, specifically excess thermodynamic properties, according to established methods for conventional liquid mixtures.[35]

The usual cosolvent mole fraction expression for simulated ChCl-based Type III DES + cosolvent systems is

$$x_{\text{cosolvent}} = \frac{N_{\text{cosolvent}}}{N_{\text{ChCl}} + N_{\text{HBD}} + N_{\text{cosolvent}}} \tag{1}$$

where $N_{\text{cosolvent}}$ is the number of cosolvent units in the system, N_{ChCl} is the number of ChCl ion pairs, and N_{HBD} is the number of DES HBD units.

A "species" fraction expression has been proposed to be appropriate for MD simulations:[81]

$$x^{\text{species}}_{\text{cosolvent}} = \frac{N_{\text{cosolvent}}}{N_{\text{Ch}^+} + N_{\text{Cl}^-} + N_{\text{HBD}} + N_{\text{cosolvent}}} \tag{2}$$

The symbols have their usual meanings except N_{Ch}^{+} and N_{Cl}^{-}, which are the numbers of choline and chloride ion units, respectively.

Finally, Kumar et al.[26] noted that the following expression may also be found in the literature:

$$x_{\text{cosolvent}} = \frac{N_{\text{cosolvent}}}{N_{\text{DES}} + N_{\text{cosolvent}}} \tag{3}$$

Here, N_{DES} is the number of DES units, i.e., ChCl plus the HBD in their eutectic (or specified) molar ratio. For example, for the prototypical DES reline, this number is the total number of 1 ChCl + 2 urea units.

Unless otherwise specified, the first cosolvent mole fraction ($x_{\text{cosolvent}}$) applies to the remainder of the text. Alternative expressions for the composition of DES + cosolvent mixtures are in use, e.g., the weight percentage (wt %), which has its usual definition, but these are less common in the computational literature.[32,33]

2.3.2. Density and Related Quantities. The most calculated property in MD simulation of IL, DES, and DES mixtures with organic solvents is the density. This property is straightforward to calculate from the trajectories and can be easily compared with the experimental data to validate the used parameters.

Density ρ is defined as mass per volume and given as

$$\rho = \frac{M_{\text{total}}}{V} \tag{4}$$

$$M_{\text{total}} = \sum_i m_i = \sum_i n_i M_i \tag{5}$$

where m_i is the mass of the component "i", n_i is the molar amount of "i", and M_i is the molar mass of "i". Density is seemingly the simplest and most fundamental property of molecular mixtures. It tells us how much mass in the solution is contained within a volume and, on a molecular level, serves as an indicator of the interactions between the components in the mixture. It is measured from experiments typically in units like g/mL, g/cm^3, or kg/m. Partial molar volume V_i of each component is an important quantity in liquid mixtures. Together with the composition of the mixture, they can strongly influence the density of the mixture when the temperature is kept constant.

For nonideal mixtures, an important quantity is the excess volume V^{E}, defined as the difference between the ideal volume and the real measured one:

$$V^{\text{E}} = V_{\text{real}} - V_{\text{ideal}} \tag{6}$$

V_{ideal}, the ideal volume of the mixture, is calculated as the sum of the volumes of the pure components, each taken in the same amount of substance as the contents are presented in the mixture. This implies that when two or more substances are mixed, the total volume is simply additive, with no volume change due to interactions between the components. In real systems, due to intermolecular forces, the actual volume of the mixture may differ from the ideal case, resulting in volume contraction or expansion.

The excess volume can be positive, suggesting that different components repel each other in this way, expanding the total volume. Positive excess volume can indicate partial immiscibility or even phase separation. If the excess volume is negative, it indicates that the unlike components attract each other more than like components, making the mixtures pack more efficiently. In general, the size of the excess volume tells us how much the mixture is nonideal. In thermodynamic modeling, excess volumes can be used to predict properties such as activity coefficients as well as the enthalpy and entropy of mixing.

In molecular simulations, the density is calculated as

$$\rho = \frac{M_{\text{total}}}{V_{\text{simulation cell}}} \tag{7}$$

The volume of the simulation cell and the number (and mass) of particles are specified by the user of the simulation software. They both are very different from macroscopic quantities measured in the laboratory, making the simulation and real conditions differ considerably. When the number of particles and volume are kept constant, we can perform simulations in a microcanonical (NVE) ensemble, where the energy is conserved, and in a canonical (NVT) ensemble, when the temperature is also constant. In both of these ensembles, the density is fixed by N and V depending on the masses of particles in the simulation cell. For complex and nonideal systems, it is difficult to get the density in a reasonable agreement with experiments. As the density depends on molecular interactions, and these are determined by the force field used, the initial box volume may not give a correct equilibrium density. In other words, it is not exactly

https://doi.org/10.1021/acs.jced.4c00505
J. Chem. Eng. Data 2025, 70, 19−43

what is obtained from experiments. Most often, it is not even known before the simulations are started. Therefore, a good protocol is to perform equilibration with a reasonable estimation of the density in the NVT ensemble and then continue in an isobaric (NPT) ensemble where the external pressure is kept constant (typically 1 atm) and the volume of the box is not fixed but can fluctuate until the box size stabilizes. This will give the working density, and the simulations can be continued in an NVT ensemble with the box dimensions obtained from the NPT simulations. The NPT simulations can also be performed using anisotropic pressures along two or three box dimensions, allowing the simulation cell to be adjusted to the simulated system. This is often used in membrane simulations.

2.3.3. Viscosity. Viscosity is one of the most studied properties of IL/DES-based systems as its high value poses a significant limitation to their applications. Unlike density, calculating viscosity in computer simulations is not straightforward. Therefore, variations in viscosity are often assessed by analyzing changes in diffusion rates using the Stokes−Einstein equation (see below).

Viscosity is a material property of a flowing liquid that strongly depends on the temperature. It measures the fluid's thickness, which arises from intermolecular interactions that create friction between molecules and resist flow (Figure 2). For example, honey is a high-viscosity, sticky fluid, while water, with a much lower viscosity, flows quickly.

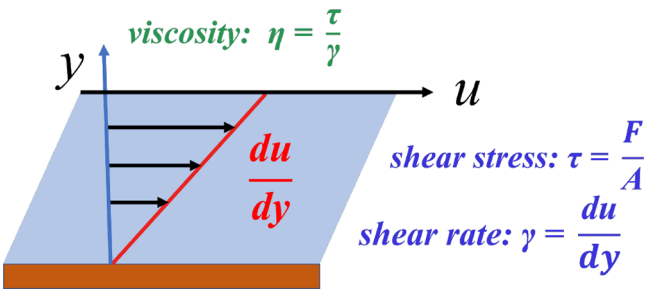

Figure 2. Viscosity (η) is quantified as shear stress (τ), given as force (F) per area (A), divided by shear rate (γ), i.e., the velocity gradient (du/dy).

The velocity along the flow direction is u:

$$\eta = \frac{\tau}{\gamma} = \frac{F}{A}/\frac{du}{dy} \tag{8}$$

The unit of viscosity is the Poise, or in SI units Pascal-second (symbol: Pa·s). Viscosity is typically expressed as either dynamic (absolute) or kinematic. Kinematic viscosity is the ratio of the absolute viscosity to density and is used to measure how quickly a fluid flows under the influence of gravity. A fluid is classified as Newtonian when its viscosity remains constant, regardless of the shear rate. Non-Newtonian fluids can exhibit nonlinear behavior, such as shear-thinning (like our blood) or shear-thickening in response to changes in shear rate. Viscosity is an important property not only in Chemistry but also in our everyday lives. For example, roughly 23% of the world's total energy consumption is lost due to friction between surfaces, even when lubricated with low-viscosity fluids.

Viscosity can be calculated from equilibrium MD simulations using the Green−Kubo formalism using the following autocorrelation function (ACF), which involves integrating over the off-diagonal elements of the pressure (shear stress) tensor:

$$\eta = \frac{V}{k_B T}\int_0^\infty \langle P_{\alpha\beta}(t)P_{\alpha\beta}(0)\rangle_{eq}\, dt \tag{9}$$

where V is the volume, k_B is the Boltzmann constant, and $P_{\alpha\beta}$ are the off-diagonal elements of the pressure calculated in MD simulations. An alternative approach (and a consistency check) is to use nonequilibrium shear flow simulations and the SLLOD method (transformation of Dolls Hamiltonian) with the Lees-Edwards sliding brick boundary conditions. For more details about equilibrium and nonequilibrium simulations of viscosity, see Sarman et al.[82] Yet another method to obtain viscosity is through the algorithm suggested by Müller-Plathe.[83]

Experimentally, viscosity can be measured using different types of viscometers, depending on the liquid and the measurement conditions.[84] Common types include capillary viscometers, which measure the flow of liquid through a narrow tube, and rotational viscometers, which measure the torque required to rotate a shaft in the liquid. Additionally, rheometers are used to measure more complex types of viscosities.

ILs and DESs are commonly high-viscosity fluids due to strong intermolecular interactions including Coulombic forces and rich H-bonding. These factors, combined with the large ion sizes, also result in a low vapor pressure. This combination currently prevents, together with high prices, the development of various technologies. Adding cosolvents is one approach to reducing viscosity, as they efficiently disrupt the long-ranged ionic networks and H-bonds, thereby enhancing mobility.[11] Water is commonly used as a cosolvent. DESs and ILs are typically hygroscopic, meaning that water can already be presented as an impurity. Organic cosolvents, whether polar, aprotic, protic, or nonpolar, such as acetonitrile, DMSO, alcohols, glycols, hexane, toluene, and acetone, can also reduce the viscosity. The choice of cosolvent and its proportion are vital areas of research, as highlighted in this review.

2.3.4. Diffusion. In liquids and solutions, the concentration of molecules is not perfectly uniform but can be considered as a mixture of crowded and less crowded smaller regions, giving rise to fluctuating concentration gradients. All molecules have thermal energy stored in their degrees of freedom, such as vibrations, rotations, and translations, that they can use for motion. The thermal motion (translation but also rotation) of the molecules is strongly hindered in condensed phases and becomes a seemingly random Brownian motion in all directions. However, molecules naturally move from more concentrated regions to less concentrated regions in their search for equilibrium. Diffusion is inversely proportional to the mass of the particle.

Einstein explained the diffusion of molecules as a "random walk" with reference to the Brownian motion of a colloid particle surrounded by a liquid of smaller molecules and gave a theoretical ground to it based on random collisions moving the large particles. Einstein did mathematically relate the mean square displacement (MSD) of particles to diffusion coefficient D:

$$^1D\colon \langle x^2\rangle = 2Dt \Rightarrow {}^3D\colon \langle \vec{r}^{\,2}\rangle = 6Dt \tag{10}$$

Einstein also found a relationship between diffusion coefficient D and the viscosity of the liquid η, temperature

https://doi.org/10.1021/acs.jced.4c00505
J. Chem. Eng. Data 2025, 70, 19−43

T, and the radius of the diffusing particle R. It is commonly known as the Stokes−Einstein equation:

$$D = \frac{k_B T}{6\pi\eta r} \tag{11}$$

Diffusion originates from random thermal motion in liquids and solutions at higher to lower concentrations. Viscosity (resistance to flow) is inversely proportional to diffusion and involves the transfer of momentum between layers of a fluid moving at different velocities. Diffusion and viscosity are transport properties, and the strong coupling between them arises from molecular interactions. Diffusion depends on the temperature and the size of the particles.

In MD simulations, the diffusion coefficient D can be calculated normally in two different ways, and both should give the same results over long enough simulations. The most common way is to use MSD by following the displacement:

$$\Delta r_i(t) = r_i(t) - r_i(0) \tag{12}$$

$$MSD(t) = \frac{1}{N}\sum_{i=1}^{N} \Delta r_i(t)^2 \tag{13}$$

This will give a graph, rising first steeply and giving a linear slope (if the graph does not rise, the liquid is frozen and nothing diffuses there). The diffusion coefficient is calculated from the slope as

$$D = \frac{1}{2d}\lim_{t\to\infty}\frac{d}{dt}MSD(t) \rightarrow d = 1,\ 2,\ 3 \text{ dimensions} \tag{14}$$

The other method is to calculate D from unnormalized velocity autocorrelation functions:

$$C_v(t) = v_i(0)\cdot v_i(t) \tag{15}$$

where $v_i(t)$ is the time-dependent translational velocity vector of particle i. The diffusion coefficient D can be obtained by integrating the VACF until it decays to zero:

$$D = \frac{1}{3}\int_0^\infty C_v(t)\,dt \tag{16}$$

When calculating the diffusion coefficient, VACF is summed and averaged over all N molecules in the system. The two methods to calculate the diffusion coefficient D, using the MSD (Einstein formula) and using the velocity autocorrelation functions and the Green−Kubo formula, can be shown to be theoretically identical.

The diffusion is often calculated when investigating the DES + cosolvents system, and among the studies reviewed here, it has been calculated by Zhang,[22] Liu,[23,24] Kumar,[26] Dawass,[27] Shah,[29] Lopez-Salas,[32,33] Wu,[38] and Panda.[43]

2.3.5. Solubility. Solubility of a solute in a solvent at specific conditions such as temperature and pressure is highly important in a wide range of applications. Among the most important are pharmaceutics, medicine, chemical engineering, and mining, as well as environmental, agriculture, and food sciences. Solubility can be defined as the maximum amount of solute that can be dissolved in a solvent. Solubility can be complete or partial, but the solute can be completely insoluble in the solvent. Experimentally, solubility can be studied by using spectroscopy when the absorbance of the solution changes. Conductometry, pH measurements, and titration can be used to determine solubility too.

In engineering modeling, there are empirical models or equations of states, parametrized on experiments. Hildebrand and Hansen solubility parameters can be used to predict solubility based on intermolecular interactions. COSMO-RS is a popular model that combines statistical thermodynamics and QC to predict solubility. MD simulations are a powerful technique for computing solvation free energies. These include thermodynamic integration, free energy perturbation, Umbrella sampling, or potential of mean force, to mention a few. The choice of method depends on the application. Often it is not easy to obtain accurate free energies of solvation due to incomplete sampling and simulations that are too short. Combining experiments and simulations will provide a deeper understanding of solubility, while simulations can also initially guide in assigning experimental studies of solubility.

2.3.6. Association and Clustering. In complex liquids, mixtures, and solutions, molecules tend to cluster and associate due to short- and long-range interactions. The same methods that are used to study solubility can be used to follow the phenomena behind association and clustering from spectroscopy (IR, Raman, UV/vis, NMR), scattering (SAXS, SANS, dynamic light scattering), and microscopies (TEM, SEM, and AFM). These studies can be combined with MD simulations (both all-atom and coarse-grained) and QC. There have been clustering algorithms developed, many of which use machine learning. The easiest method for simulations is to analyze radial distribution functions.

2.3.7. Probability and Distribution Functions. Probability and distribution functions are essential tools to study the densities of atoms and molecules to learn how they are organized in space and time and how they interact in condensed phases. Below, we give examples of several functions that can be used to study DES systems.

2.3.7.1. Radial Distribution Function and Related Quantities. Radial distribution functions (RDF), a.k.a. pair correlation functions, have kept their position as fundamental tools in studies of molecular liquids and solutions from the early days of liquid theories.[85] From RDFs, it can be quickly read how a particle density varies as a function of distance from a reference particle. Experimentally, RDFs can be obtained from the data of scattering studies (X-ray, neutron, and electron). Before particle-based computer simulations, integral equations theories were developed connecting pair correlation functions to pair potentials.[86] From the days of very early computer simulations by Alder and co-workers, RDFs are routinely calculated from trajectory data for all types of systems, from simple liquids to ILs and biomolecular systems.

In studies of the liquid structure of these neoteric liquids, the most powerful methodology is to combine molecular modeling and simulations with experiments. From MD simulations (also Monte Carlo), the structure can be determined by calculating radial distribution functions (RDF) $g(r)$ between selected pairs of atoms in the simulated system. The same information can be obtained from small-angle X-ray scattering (SAXS) and small-angle neutron scattering (SANS) as the scattering structure factors $S(k)$. These are functions of reciprocal distance ($k = 1/r$), so after Fourier-transforming and separating them from total structure factors to partial structure factors, they can be compared with the real space functions RDFs. RDFs between two types of atoms A and B can be calculated from MD (or MC) trajectories as

https://doi.org/10.1021/acs.jced.4c00505
J. Chem. Eng. Data 2025, 70, 19−43

$$g_{AB}(r) = \frac{\rho_B(r|r_A = 0)}{\rho_B} \tag{17}$$

which gives the conditional probability to find atom B at a distance r from atom A. Note that the function is normalized by the bulk density of B in the studied system. Note that when $g(r)$ is properly normalized, it should approach one at long distances corresponding to the bulk density. The corresponding structure factor $S_{AB}(k)$ can be calculated from the normalized $g_{AB}(r)$ as

$$S_{AB}(k) = \frac{N_A}{N}\left\{\delta_{AB} + \frac{N_A}{V}\frac{4\pi}{k}\int_0^\infty [g_{AB}(r) - 1]\sin(kr)r\ \mathrm{d}r\right\} \tag{18}$$

Another important quantity, calculated from $g(r)$, is the potential of the mean force (PMF), which gives the effective interaction between two particles. PMF can provide free energy when integrated along a reaction coordinate between two states. Denoted as $W(r)$, it can be given as

$$W(r) = -k_B T \ln g(r) \tag{19}$$

where k_B is the Boltzmann constant (in J/K), and T is the temperature (in K). Negative $W(r)$ means attraction, while positive means repulsion. PMF as such can describe only pairwise interactions as many-body effects do not enter into $g(r)$.

The significance of this type of analysis is evident as RDF calculations are a fundamental component in nearly all MD simulation studies of DESs + NATC discussed in this review.

2.3.7.2. Coordination Numbers. A very useful unitless single-number quantity in solution studies is the coordination number or solvation number (n), which is called the hydration number when obtained from aqueous solutions. To obtain it from MD simulation data, it requires regular first calculations of RDFs, giving the probability to find the closest solvent molecules around a solute molecule, ion, or atom in a larger solute. Typically, in the RDF, the entire first peak (maximum) to the bottom of the first minimum gives the first solvation shell (or hydration shell if water is the solvent). If the first maximum is relatively high (for example >3 in the intensity of a normalized RDF), it tells that the solvent molecules interact strongly with the solute, forming a strong solvation shell. Typical examples are ions and charged solutes. In these cases, the first minimum also approaches zero in intensity, which in turn is a measure that there is a very slow exchange of solvent molecules between the solvation shell and the bulk. If there is a fast exchange, the first maximum is broad, and the first minimum is less deep and not approaching zero intensity.

A running coordination number to any distance from the reference point in the solute can be calculated from

$$n(r) = 4\pi\frac{N}{V}\int_0^R r^2 g(r)\ \mathrm{d}r \tag{20}$$

where $n(r)$ is the distance-dependent coordination number, and N/V is the bulk number density of the solvent molecules. If R is fixed to the distance of the first minimum of the RDF, then the equation above gives the population of the solvents in the first solvation shell. Note that the coordination number does not need to be an integer like 4, 6, etc., but will most likely be a rational number like 3.7 or similar. This is simply because there can be solvent molecules not very tightly bound to the solute so they can easily go to the bulk while a new solvent molecule can take their place in the solvation shell. If the solvation shell is very tight due to strong solute−solvent interactions, there can be a second or even third solvation formed while successively weaker. For example, water molecules have three distinct hydration shells like an onion, which becomes clear from $g(r_{OO})$. Note also that for large solute molecules, the solvation shells are fractionated but the RDFs can be used equally well to calculate the coordination number. The coordination number given above, when calculated from plain RDF, depends only on the distance. If preferred orientations of the solvent molecules are of interest, angular parameter(s) can be added in the distribution function, such as $g(r, \theta)$, and the coordination number is calculated as

$$n = 4\pi\frac{N}{V}\int_0^R r^2\int_0^\pi g(r, \theta)\sin\theta\ \mathrm{d}r\ \mathrm{d}\theta \tag{21}$$

Coordination numbers can be obtained either directly or indirectly using several experimental techniques and can be used as complementary information to computer simulations. Diffraction (X-ray, neutron, and electron) can provide total and partial structure factors (see subsection for RDF) from which RDFs (and coordination numbers) can be deduced. Hydration numbers can sometimes be obtained from NMR relaxation studies. Also, coordination numbers can sometimes be estimated from (shifts and intensities) vibrational spectroscopy.

2.3.7.3. Hydrogen Bonding Analysis. The study of H-bonding is important for understanding the molecular origin of many processes in areas from chemical engineering to biology. H-bonds are not only structural constellations but are equally dynamical. H-bonds are an essential component, stabilizing many biomolecular systems. Many methods can be used to gain information about forming and breaking H-bonds, including their strengths and lifetimes. Spectroscopy, including NMR, IR, Raman, and UV/Vis, provides information about characteristic frequency shifts caused by H-bonding events. The strengths and nature of H-bonds can be studied from changes in the electronic states. Also, X-ray (small angle) and neutron scattering are important sources of H-bonding for highly structured liquids. Calorimetric techniques, such as isothermal titration and differential scanning calorimetry, can measure heat changes upon H-bonding events.

QC methods are ideal for studying H-bonding on a molecular level and how the electronic states are affected. QC gives direct binding energies and geometries from H-bonded moieties. In modeling, MD simulations (both force-field-based and ab initio) are ideal techniques to study both the structure and dynamics of H-bonding. The insight can be obtained by combining experiments, theory, and simulations.

Commonly applied criteria for H-bonds of X-H···Y are where X and Y = O, N, S, F, Cl and where Cl is an electronegative atoms. The dotted line is the H-bond and the solid line covalent bond. Typically, a geometric criterion is applied, the donor (X)−acceptor (Y) distance is in the order of 2.5−3.5 Å, and the X−H−Y angle is 150−180 deg. In MD simulations, H-bonds are formed by atomic charges. Indeed, H-bonds are predominantly of electrostatic (Coulombic) origin. In some cases, a special type of short-range potential is added to the electrostatic potential:

$$U_{\text{H-bond}} = \frac{A}{r^{12}} - \frac{B}{r^{10}} \tag{22}$$

https://doi.org/10.1021/acs.jced.4c00505
J. Chem. Eng. Data 2025, 70, 19−43

which constrains the H-bond distance. Also, another term to constrain the angle can be used. With the above criteria, the H-bonds can be counted during the simulations, which then can be averaged. Typically, a H-bond correlation function can be created from the trajectories:

$$C_{HB}(t) = H(0)\cdot H(t) \tag{23}$$

where $H(t)$ is a binary 1 or 0, with "1" indicating an H-bond according to some used criterion. This correlation function gives the residence times from averaged periods of 1 digit. It can also be used to detect intermittent lifetimes when the H-bond is temporarily broken but reformed again.

Radial distribution functions can readily give information on weak and strong H-bonds, giving also the average H-bond distance. Many common simulation software comes with analysis tools for H-bonds, including long-ranged topologies.

2.3.7.4. Spatial Distribution Function. Due to their strong interactions, the liquid structures of ILs and DESs show exceptionally long lifetimes to form short- and long-ranged aggregates and structural correlations. Another very powerful methodology can be applied to obtain their three-dimensional liquid structure. While $g(r)$ only shows the liquid structure radially, the so-called spatial distribution functions (SDF) can provide fully 3D probability images[87] not only around reference atoms but also reference molecules. They can be calculated from the MD trajectories as

$$g_{AB}(\vec{r}) = \frac{\rho_B \vec{r}|\vec{r}_A = 0}{\rho_B} \tag{24}$$

Note, instead of plain distances between reference atom A and all atoms B, we use vectors that are calculated in molecular coordinates of the reference molecule where atom A is attached. The distance vectors provide both the directions and distances to probability densities of neighboring atoms, thereby giving a 3D structure when averaged over equilibrated trajectories. As an illustration of how powerful SDFs are in providing insight into the complex structure of DESs and ILs, we show the cosolvent water structure around four ILs in Figure 3.

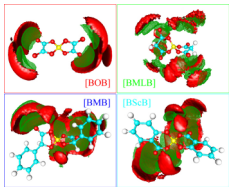

Figure 3. Spatial distribution functions between water (red solid surface oxygen, green meshed surface hydrogen) and four orthoborate anions: bis(oxalato)borate ([BOB]), bis(malonato)borate ([BMLB]), bis(mandelato)borate ([BMB]), and bis(salicylato)borate ([BScB]) from simulations with the trihexyltetradecylphosphonium cation [$P_{6,6,6,14}$]. Reprinted with permission from ref 88. Copyright 2016 AIP Publishing.

In Figure 3, the coordinate system is fixed on the ILs while the most probable positions of water oxygen and hydrogen, obtained from MD simulations, are shown around. Obviously, SDFs may not always be as straightforward to construct as RDFs, as they require relatively stiff reference molecules to construct the local frame and also require much longer simulations to obtain noiseless SDFs. SDFs are widely used in the field of IL-derived chemical systems and simulation software such as Tranal (Trajectory Analysis module to M. DynaMix MD simulation package[89]), and Travis[90,91] can be used to calculate them. To visualize them, for example, VMD[92] or gOpenMol[93] can be used.

2.3.8. Excess Thermodynamic Properties. Both in chemistry and chemical engineering, different excess properties play a crucial role in understanding and modeling liquid mixtures deviating from ideal behavior, especially under nonideal conditions. Among the most important are:

- Excess Gibbs energy (G^E): this is the most important property in solvation chemistry as it can be directly related to activity coefficients. It is used to describe phase equilibria, particularly vapor−liquid equilibrium. DESs contain strong interactions, including H-bonds. Knowing G^E is useful in applications such as extraction and separation.
- Excess chemical potential (μ^E): directly related to G^E,μ^E serves as a driving force for mass transfer. In solvent extraction with DESs, understanding μ^E can be used to improve the selectivity and efficiency of these processes.
- Excess enthalpy (H^E): this is a measure of the heat effects during the mixing of liquids. It is the key quantity in designing efficient heat exchangers. Due to the strong interactions, DESs show large heats of formation. Detailed knowledge of H^E is important in the design of heating and cooling systems containing DESs.
- Excess entropy (S^E): this quantity helps us to understand the aspects of randomness in mixing, not at least in the configurational degrees of freedom. It is an important property in studies of complex fluid mixtures and, in particular, those containing polymers. Understanding S^E is important in predicting the temperature-dependent behavior of DESs.
- Excess volume (V^E): V^E is important in understanding changes in the density and compressibility of liquid mixtures. It is critical in numerous processes with flows of liquid mixtures.
- Excess viscosity (η^E): this is a highly relevant property for DESs in particular for their flow behavior. DESs have normally higher viscosities than their individual components, slowing the mass transfer and affecting mixing in important processes with them.
- Excess conductivity (κ^E): this quantity helps in understanding ionic transport properties of DESs, important in both separation and electrochemistry with batteries and capacitors, where it can be the key performance parameter.

The experimental measurement of excess thermodynamic properties, e.g., the molar enthalpy of mixing, denoted H_m or ΔH_{mix}, or the excess molar volume, V^E, provides information about changes in intermolecular interactions and molecular arrangements that occur upon mixing of two liquids.[11] These properties can also be computed from MD simulations and serve as a means of verification of simulations against experiment.

The V^E values of simulated mixtures are calculated according to the following equation:

$$V^E = \frac{x_1M_1 + x_2M_2}{\rho_{mix}} - \frac{x_1M_1}{\rho_1^*} - \frac{x_2M_2}{\rho_2^*} \tag{25}$$

https://doi.org/10.1021/acs.jced.4c00505
J. Chem. Eng. Data 2025, 70, 19−43

where x_1 and x_2 are the mole fractions of the two mixture components, M_1 and M_2 are their molecular weights, ρ_1* and ρ_2* are the simulation average densities of the components in their pure state under identical conditions, and ρ_{mix} is the simulated density of the mixture.[11]

The mixing enthalpy associated with the combination of two liquids is calculated from MD simulations as the excess molar enthalpy, H^E, using the formula:

$$H^E = U_m - x_1U_1 - x_2U_2 + PV^E \quad (26)$$

with U_m the average potential energy per molecule in the simulated mixture, U_1 and U_2 are the average potential energies per molecule of the pure components, P is the pressure, and V^E the excess molar volume defined above.[94] The PV^E term makes a small contribution to the H^E for liquid mixtures and is often omitted from the calculation.[95] The calculation of H^E for simulated Type III DES + cosolvent mixtures is complicated by the fact that these DESs are themselves mixtures, and one of their components (ChCl, or another quaternary ammonium salt) is dissociable.[35]

2.3.9. Preferential Solvation and Cosolvent Effects. If a solute in a solvent mixture interacts more strongly with one of the components, then we can speak about preferential solvation. Typically, some salts can be solvated preferentially in mixed solvents. In more extreme cases, a solute cannot be solvated in any of the pure components of the mixture but readily in the mixture of them at a certain composition. In MD simulations, these phenomena can be seen and studied, for example, by calculating solute−solvent RDFs or SDFs and analyzing them closely. Mixed solvent effects can occur in DESs typically when one component is a HBD, and the other is a HBA. The DESs can form H-bonded networks where a suitable solute can perfectly fit and be part of the network. However, the mixed solvent effects can also take place with interactions (charge, dipole, etc.) involved other than H-bonding.

A typical example is DES made of ChCl (HBA) and urea (HBD), where an ionic solute would preferentially interact with chlorides of ChCl via electrostatic interactions. While an organic solute would prefer to interact with urea.[96,97] All of these combinations of possible interactions will lead to unique solvation environments, very different from what we are used to observing in solvation chemistry. We need to learn to understand these effects in order to design novel processes. Computer simulation methods are ideal tools for studying complex solvation phenomena.

2.3.10. Distribution Coefficient. Distribution coefficient or partition coefficient $K_D = C_1/C_2$ is a commonly used concept in chemistry, used in liquid−liquid extraction or distribution of solute molecules between two immiscible liquid phases "1" and "2", where C is the dissolved concentration. Similarly, how to partition a solute in two phases where one is DES and the other is a traditional (water or organic solvent), the distribution coefficient is given as

$$K_D = \frac{[solute]_{DES}}{[solute]_{other\ phase}} \quad (27)$$

The distribution coefficient is a critical parameter, revealing the efficiency, selectivity, and overall performance of DES in liquid−liquid extraction. As a highly tailorable system, the DES in question can be tuned for specific applications in green chemistry, environmental science, and pharmaceutics. Larger D means higher preference for the solute to be found in the DES phase.

Liu et al.,[23,24] in their MD simulation studies of the extraction of alcohols from fuel by common Type III DESs, made use of the following distribution coefficient (K_D) formula:

$$K_D = \frac{x^E_{alcohol}}{x^R_{alcohol}} \quad (28)$$

In the above equation, x^E and x^R are the mole fractions of alcohol in the extract (DES) and raffinate (fuel) phases, respectively. The authors also define the extraction selectivity, S, as follows:

$$S = \frac{\beta_{alcohol}}{\beta_{alkane}} = \frac{x^E_{alcohol}/x^R_{alcohol}}{x^E_{alkane}/x^R_{alkane}} \quad (29)$$

where the alkane refers to the alkane employed as fuel model (i.e., the raffinate/fuel phase).

2.3.11. Properties Calculated from QM Methods. The first molecular properties calculated using QC are most likely the optimized molecular geometry and structure including bond lengths and angles. Already this information can tell us how the molecules interact with other molecules like solvents. Also, steric effects together and conformations for flexible molecules. For scientists doing molecular simulations, the charge distribution and dipole moment are important in understanding how the molecule interacts with polar molecules and if it can create H-bonds. In going further, polarizability is key information, telling about the electron clouds and how easily they can be distorted. High polarizability often indicates stronger van der Waals interactions, which in turn influence the solvation dynamics. All of these are examples of molecular properties. Next, we can calculate different types of interaction energies, such as solvation energy, by transferring a solute from the gas phase into a solvent to predict solubility. We can calculate interaction energies in H-bonding situations, electrostatic and van der Waals interactions, binding energies in complex forming, etc.

Many spectroscopic properties can be calculated, including solvent effects in electronic transitions and vibrational frequencies, NMR chemical shifts, and coupling constants. We can get good estimations of thermodynamic properties such as entropy and enthalpy of solvation and also free energy. Continuum solvation models can be employed for the solvent effects. Other properties of interest are pK_a values for acid−base equilibria.

2.3.11.1. Molecular Electrostatic Potential. The molecular electrostatic potential (MEP) is a key concept in computational chemistry used to characterize a molecule's charge distribution. The MEP indicates the potential energy that a positive test charge would experience at different points around a molecule. This potential is shaped by the arrangement of the nuclei and the electron distribution within the molecule. MEP maps are frequently used to identify regions of a molecule that are either more electron-rich or -poor, aiding in the prediction of how the molecule might interact with other species, including ions, molecules, or solvents.

These maps are particularly useful for analyzing molecular recognition, reactivity patterns, and intermolecular interactions such as H-bonding and van der Waals forces.

In the field of ILs, DESs, and their mixture, MEPs are typically obtained from DFT calculations and are of great

https://doi.org/10.1021/acs.jced.4c00505
J. Chem. Eng. Data 2025, 70, 19−43

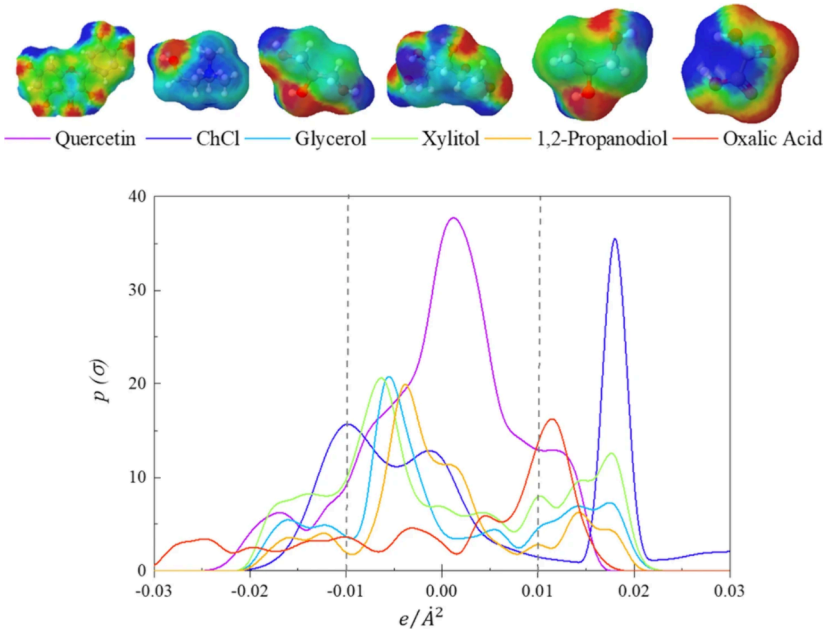

Figure 4. Top: MEP of ChCl and other organic molecules. Bottom: Corresponding σ-profiles. The region on the left of the σ-profile is related to the H-bond donor capability, the central is the nonpolar contribution, and the right region is related to the H-bond acceptor capability. Reprinted with permission from ref 98. Copyright 2023 Springer Nature.

benefit to understand the complex bonding pattern of the complex mixtures. See, for example, the studies of Dai et al.[25]

2.3.11.2. Interaction Region Indicator. A recently developed function that allows to visualize different types of interaction within a chemical system is the Interaction Region Indicator (IRI).[99] The IRI is a real space function designed to visually reveal both chemical bonds and weak interactions within chemical systems. It offers a simple expression that is easy to calculate, and its graphical representation effectively illustrates interatomic interactions across a wide range of chemical systems. IRI can be calculated using electron density data from either QM calculations or high-resolution X-ray diffraction. Examples of applications can be found in the studies of Dai et al.[25]

2.3.11.3. Chemical Potential. Chemical potential μ in QM is related to the electronic properties, such as the highest occupied molecular orbital (HOMO) energy, ionization potential, and electron affinity. It can be calculated using ionization potential (IP) and electron affinity (EA) of the molecule:

$$\mu = -\frac{1}{2}(IP + EA) \tag{30}$$

where IP is the energy required to remove an electron from the molecules, while EA is the energy released when an electron is added to the molecule.

2.3.11.4. σ-Profile Analysis. The σ-profile is a key concept in the COSMO-based models. It provides a simplified representation of the charge distribution on the surface of a molecule, which can be depicted in two dimensions: the x-axis typically represents the surface charge density (σ), while the y-axis indicates the relative amount of the surface corresponding to each charge density. Figure 4 shows examples of σ-profiles for several organic molecules, along with their corresponding MEPs.

The σ-profiles obtained with the COSMO models have been successfully employed by several studies involving DES + NATCs. See in the following, the investigation of Dai et al.[25] on separating azeotropic MTBE + MeOH mixtures; Sun et al.'s[28] testing of DESs and ILs for the separation of ethyl acetate and IPA; Deng et al.'s[39] work on extracting sulfurous compounds from fuel oil; and Wu et al.'s[38] study on the separation of phenol from oil mixtures.

2.3.11.5. Natural Bond Orbitals (NBOs). NBOs are a concept in QC to describe the bonding in an intuitive and natural way focusing on bonding, nonbonding pairs and lone-pairs rather than delocalized molecular orbitals (MO).[44−46] This way, they use the more commonly known σ and π bonds. They can also be used to analyze the electron distribution, thereby providing insights into partial charges that are not observable in molecular QM. In an NBO analysis, the donor−acceptor interactions can be calculated in a conceptually simple way. NBOs are important in better understanding bonding in complex molecular structures such as the DES systems with charge transfer. They can also help in predicting the reaction pathways. But after all, they are useful in analyzing H-bonds.

NBOs are constructed by starting from wave functions obtained in conventional QM calculations (Hartree−Fock, DFT, MP2 or coupled cluster), giving molecular orbitals (MOs). The MOs are expressed in atomic orbitals, which are ortho-normalized and transformed to natural atomic orbitals (NAO) and thereafter combined to NBOs. This involves the formation of both bonding and lone-pair NBOs. A natural population analysis (NPA) can be performed to quantify the distribution of the electron density. In NPA, the electron density is projected onto NAOs and the occupancy (number of electrons) of each NAO is determined and summed to give a natural population of each atom. The difference between the nuclear charge and the natural population gives the atomic charge. All of this can be facilitated with main-stream QC software packages. The purpose of NBOs is to have a chemically intuitive picture of bonding and electron distribution.

https://doi.org/10.1021/acs.jced.4c00505
J. Chem. Eng. Data 2025, 70, 19−43

2.3.11.6. Atoms-in-Molecule (AIM). A similar concept to natural bond orbitals (NBO), in a sense to give a more intuitive picture of electron density in molecules, is the "Atoms In Molecules" (AIM), which is related to chemical bonding, molecular structure, and reactivity.[44−46] AIM is based on the basic quantum mechanical observable, electron density $\rho(r)$, within a molecule and to analyze it to find critical points, where its gradient is zero. These points are typically found, for example, at the sites of nuclei between two bonded atoms and ring structures. Zero gradients can be used to define clear boundaries between atoms within molecules. Various properties for atoms can be calculated such as their charges and volumes, but some properties of bonds can also be obtained from electron density at bond critical points (BCPs). AIM analysis normally requires specific software tools that some mainstream QC packages offer. The purpose of an AIM analysis is to gain an understanding of how the electronic structure and electron density can provide a picture of atoms and how they contribute to bonding, structure, and reactivity. The analysis is valuable in organic and biochemistry to study how substituents affect bond strengths and reactivity, while in inorganic chemistry coordination compounds can be analyzed.

3. DISCUSSION ON COMPUTATIONAL STUDIES OF DES COSOLVENT MIXTURES

After the overview of computational models and methods to study DESs in general, but focusing on them with cosolvents and, in particular, cosolvents other than water, we now review and discuss the work found in the literature to date (May 2024). The very reason to review the field is to present the work done by modeling and simulations to give a better molecular understanding of these highly complex systems. However, modeling is not just the best method to study detailed structures and processes created by complex spectrum short- and long-range interactions, it is the only method. When combined with models used in chemical engineering and advanced experimental techniques, this provides an integrated methodology for future innovations.

In this section, we review and discuss, to date, published investigations, applying QM and MD simulations to understand and predict the properties of DES + NATC.

3.1. Physico-chemical and Thermophysical Properties. Characterizing and rationalizing the thermophysical, physical, and physicochemical properties, such as conductivity, viscosity, density, melting points, and excess properties, are of crucial importance for their application. As noted by Cea-Klapp et al.[34] "...the understanding and modeling of thermophysical properties of DESs are still a rough and unexplored terrain, mainly for the complexity of their hydrogen-bonding interactions." While this affirmation is still actual, and during the past few years, there have been several notable studies.

Cea-Klapp et al.[34] investigated the thermophysical and transport properties of methanol mixtures with reline and glyceline. They compared density, excess molar volume, and viscosity predictions from PC-SAFT modeling and classical MD simulations with experimental data, focusing on the role of H-bonding interactions. The study reported good agreement among MD simulations, PC-SAFT modeling, and experimental thermophysical properties. Interestingly, to the best of our knowledge, no prior calculations of the excess volume from MD simulations of ChCl-based DES + NATC mixtures had been reported before this publication. RDFs and H-bond analyses from MD simulations revealed that the incorporation of methanol does not significantly alter the interactions in the original DESs, though methanol strongly competes with a secondary HBD. The interactions between DES HBDs and methanol were also found to be important. These findings highlight the complexity of molecular associations in these systems and underscore the challenges in modeling and predicting their properties.

The excess molar enthalpies (H^E) of ethaline mixtures with water and methanol have been found to be of opposite sign, those of water mixture being strongly negative and those of methanol positive, suggesting that while both cosolvents reduce the DES viscosity, the changes in intermolecular interactions associated with mixing are different.[20] Engelbrecht et al.[35] performed MD simulations aimed at reproducing and rationalizing the experimental H^E trends for these systems. Since no previous calculations of DES + cosolvent excess molar enthalpies were reported at the time of publication, the correct approach for calculating this property from MD simulations of these complex systems was not immediately clear.

Two variations of the approach typically used for the related DESs were tested, and both satisfactorily reproduced the experimental H^E data (Figure 5A). Importantly, the experimental H^E sign difference was reproduced. Structural analyses based on RDFs involving the DES chloride anion and corresponding coordination numbers allowed for rationalization of the H^E sign difference due to strong water-chloride interactions, with water inserting between neighboring chloride anions, forming ionic H-bonded bridge structures. While

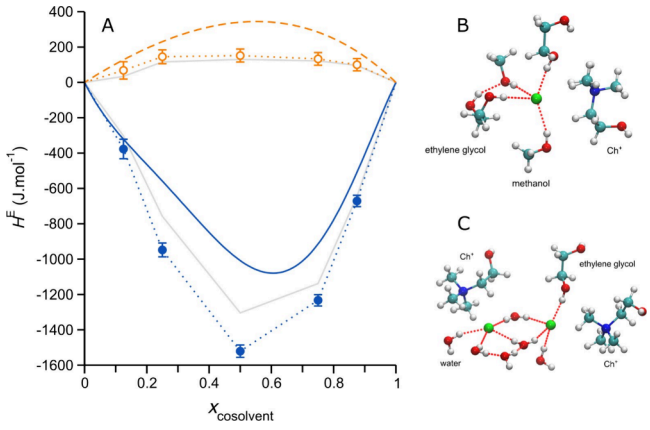

Figure 5. (A) Excess molar enthalpies, H^E(J/mol), of ethaline + water (blue data) and ethaline/methanol (orange data), were obtained from simulation and experiment. The smooth blue solid and dashed orange lines are nonrandom two liquid (NRTL) fits to the experimental data reported by Ji and co-workers.[20,100,101] Simulated data are shown in blue solid circles for water mixtures and open orange circles for methanol mixtures; these data are connected by dotted lines to guide the eye. The results from an alternative approach to calculating H^E from the MD simulations are shown in solid light gray lines. (B) Representative Cl^- coordination shell configurations were obtained from simulations of equimolar DES + methanol mixtures. (C) As in B, for the DES + water mixture. Water molecules form strong −O−HCl− H-bonds between neighboring Cl^- anions, resulting in compact water-bridged structures with a characteristic interionic separation that gives rise to the $g_{ClCl}(r)$ first maximum at ∼5 Å; water molecules also self-associate via strong H-bonding. Methanol molecules are unable to form such H-bonded bridges between Cl^-. Adapted with permission from ref 35. Copyright 2022 Engelbrecht, Ji, Carbonaro, Laaksonen, and Mocci.

https://doi.org/10.1021/acs.jced.4c00505
J. Chem. Eng. Data 2025, 70, 19−43

methanol is also able to form H-bonds with chloride, it cannot support a similar H-bonded network and effectively disrupts the native DES H-bonded network when competing with ethylene glycol as HBD. See Figure 5B,C for examples of coordination geometries. While both water and methanol reduce the DES viscosity, and the H-bond characteristics of these mixtures may have important implications for potential applications. ILs and, more recently, DESs have attracted considerable attention as both media and catalysts, as well as supporting components of catalysts, for the electrochemical processes, and particularly, for CO_2 reduction reaction (CO_2RR).[102] This interest is due to their unique advantages in reducing the overpotential, enhancing product selectivity, and offering customizable properties. To assess the feasibility of DES solvent systems for such applications, it is first necessary to study their thermophysical properties, as well as those of the solutions of interest, i.e., containing the reactants and products. Knowledge of the solubility and diffusivity of these solutes is particularly important. Dawass et al.[27] performed MC and MD simulations to screen two DESs, reline and ethaline, along with their mixtures with MeOH or PC, as potential media for the electrochemical reduction of CO_2. The MC-derived Henry coefficients of CO_2 in ethaline + cosolvent mixtures were comparable to those in the pure cosolvents MeOH and PG, both of which are commonly used as solvents for electrochemical reduction. In the reline mixtures, the coefficients were slightly lower yet still indicate acceptable CO_2 solubility. Additionally, the solubilities of both reduction products, oxalic and formic acid, were higher in the DES mixtures than in the pure cosolvents. For the DES + cosolvent mixtures, the MD-derived densities were consistent with experimental data, as were the viscosities with the available experimental values (Figure 6).

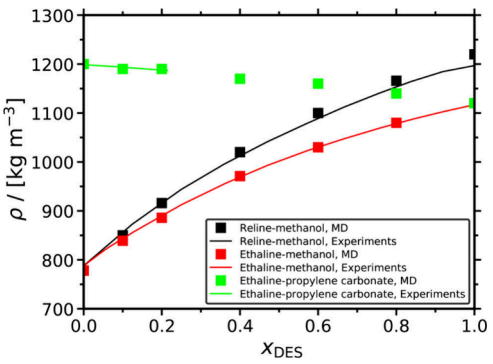

Figure 6. Experimental and computed viscosities of DES + cosolvent mixtures as a function of the DES mole fraction. The red and green lines connect previously published experimental data for ethaline + methanol[20] and ethaline + propylene glycol,[103] respectively. Reprinted with permission from ref 27. Copyright 2022 American Chemical Society.

The self-diffusion coefficients of the mixture components decreased monotonically with an increasing DES content. H-bond analysis revealed that MeOH significantly impacts the number of H-bonds between DES components by forming new H-bonds with them. In contrast, PG is unable to form H-bonds with the DES anion and does not affect the DES H-bonding interactions to the same extent. The computed electrical conductivities displayed a nonmonotonic dependence on composition: they increased with the addition of DES to the cosolvent, peaked at a certain point (different for two DESs), and then decreased as the viscosity rose. The authors conclude that mixtures with low DES content are the most practical for electrochemical applications due to their high conductivity, low viscosity, and good CO_2 absorption capacity.

3.2. Extraction Studies. DESs are promising green solvents for use in liquid−liquid extraction (LLE) and MD simulations are increasingly used to model this process and rationalize the extraction mechanisms at the molecular level. However, until recently, only a few computational studies of DESs as extractants in LLE had been reported.[104] Wang, Cui, and co-workers were among the first to apply MD simulations to investigate the extraction of various alcohols from their mixtures with *n*-hexane using ChCl-based DES.[22−24] They began by performing classical MD simulations to explore the LLE mechanism of 1-butanol separation from an *n*-heptane + 1-butanol azeotropic mixture using prototypical Type III DESs: reline, ethaline, glyceline, and ChCl + propylene glycol 1:2.[22] The MD simulations effectively modeled the entire LLE process for each DES, confirming the experimental 1-butanol extraction efficiency trend: reline has the best extraction effect, while 1:2 ChCl + propylene glycol has the worst.

An analysis of interaction energies during the simulations further supported the LLE effect trend, showing that all DESs considered exhibit high selectivity for 1-butanol over *n*-heptane (Figure 7).

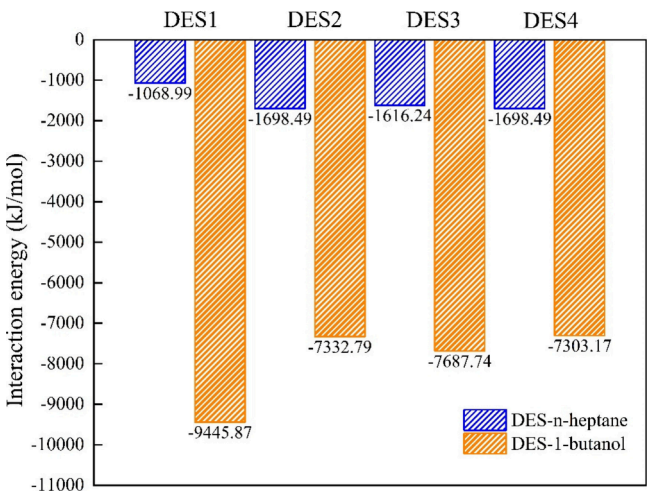

Figure 7. MD nonbonded interaction energies between DESs and 1-butanol (orange) and *n*-heptane (blue). DES1: reline; DES2: ethaline; DES3: glyceline; DES4: ChCl + propylene glycol 1:2. Reprinted with permission from ref 22. Copyright 2021 Elsevier.

For all DESs, the chloride anion was found to play a dominant role in 1-butanol extraction due to strong H-bonding interactions. However, an analysis of RDFs and SDFs revealed similar interactions between ChCl and 1-butanol in all the studied DESs, suggesting that the HBD is directly responsible for the observed difference in the 1-butanol extraction effect.

In a subsequent study, the same group[23] extended their approach by investigating how reline, ethaline, and glyceline form biphasic systems when contacted with MeOH-*n*-hexane azeotropic mixtures and can be used to efficiently extract MeOH from these mixtures. The different efficiency of the studied DESs was evaluated by calculating MeOH distribution coefficient and selectivity. As in the previous study,[22] the authors performed MD simulations to study the entire MeOH

https://doi.org/10.1021/acs.jced.4c00505
J. Chem. Eng. Data 2025, 70, 19−43

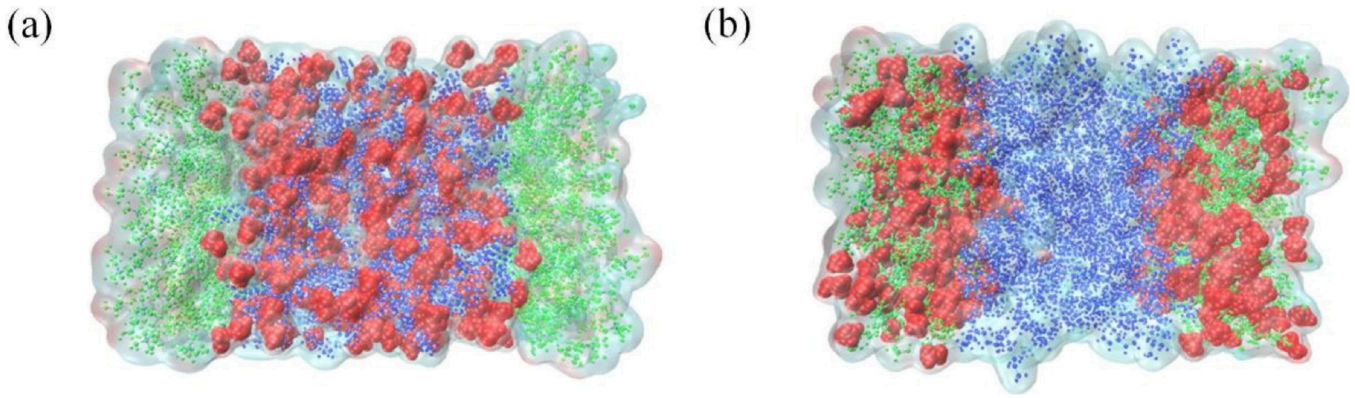

Figure 8. Snapshots of biphasic MD simulation systems: (a) before and (b) after MeOH extraction. Color code: DES in green, *n*-hexane in blue, and MeOH in red (space-filling representation). Reprinted with permission from ref 23. Copyright 2022 Elsevier.

extraction process by these DESs from the *n*-hexane phase (Figure 8).

The computed MeOH distribution coefficients aligned well with experimental data, reproducing the experimental MeOH extraction effect trend: ethaline > reline > glyceline. An analysis of interaction energies between components during the MD simulations showed that electrostatic interactions are the main driving force in MeOH extraction by the DESs.

A structural analysis using RDFs and SDFs further revealed the DES chloride anion to be the primary interaction site for extracted MeOH molecules; the DES HBD plays a more subtle but definite role, with ethylene glycol interacting more favorably with MeOH. In a parallel investigation, the same MD and analysis protocols were applied to study the extraction (with the same DESs) of the higher-alcohol fuel additive IPA from an *n*-hexane mixture.[24] Nonbonded interaction energies, IPA distribution coefficients, and IPA/*n*-hexane selectivities computed from the MD simulations corroborated experimental results, indicating that ethaline performs best in this LLE application. The authors investigated the effect of the IPA + *n*-hexane azeotropic ratio on the IPA extraction efficiency of ethaline, finding a decrease with increasing IPA content. An analysis of simulated structural (RDFs, SDFs) and dynamic (mean squared displacement)[23] HBA, readily forming H-bonds with MeOH. MEP and IRI analyses confirmed strong H-bonding interactions between the chlorine atoms of ChCl and the hydrogen atoms in the hydroxyl group of MeOH, while MTBE exhibited weaker van der Waals interactions with DES molecules. By analyzing RDFs, SDFs, and nonbonded interaction energies in MD simulations, it was shown that the extraction process of MeOH using ChCl-based DESs primarily relies on these H-bonding interactions. Based on the molecular modeling predictions, three DESs (ChCl-1,4BDO, ChCl-1,3PDO, and ChCl-urea) were selected for LLE experiments. The experimental results validated the computational findings, with ChCl-1,4BDO demonstrating the best performance for MeOH extraction, as indicated by its highest allocation coefficient. In contrast, ChCl-urea exhibited superior selectivity, effectively reducing MTBE waste. To assess the feasibility of DES extraction for industrial applications, the authors simulated an extraction process involving ChCl-1,4BDO using Aspen Plus V11. The simulation indicated significant economic and environmental benefits compared with an extractive distillation process, with a 50.3% reduction in steam consumption and a 38.9% decrease in total annual cost. DFT calculations were further employed in the subsequent work of Wang's group[28] to understand and optimize the extraction of IPA from an azeotropic mixture with ethyl acetate (EAC). Different solvents were evaluated for the extraction: three ILs based on 1-ethyl-3-methylimidazolium [EMim] with three different counterions ([AC], [H_2PO_4], and [HSO_4]) and the DESs ethaline, glyceline, reline, and the mixture ChCl:MA (1:2). σ-profiles of all the molecules involved in the extraction were obtained with the COSMO-SAC models and used to verify the H-bonding capabilities and rapidly screen the extractant efficiency. The DES configurations were obtained with Molclus software,[105] and the MEPs derived from QM calculations on DESs, ILs, IPA, and EAC were used to determine the best relative orientations of molecules in the IL/DES-IPA complexes. Subsequently, electron density differences, mutual penetration distance, the independent gradient model based on the Hirshfeld partition (IGMH), bond critical points and H-bonding energy were calculated within the framework of AIM theory.[106] These analyses provided valuable insights into the extraction mechanisms and allowed for assessing the efficiency of IL and DES, offering a valuable prediction of extraction capabilities, which were confirmed by LLE experiments. Among the DESs, the ethaline-IPA complex showed a larger mutual penetration distance (1.23 Å) than that of EAC-IPA (1.09 Å), indicating stronger intermolecular forces, which are crucial for the extraction process. Reline-IPA and glyceline-IPA had smaller values, indicating a lower efficacy in extracting IPA. In contrast, the ChCl + malonic acid mixture (1:2) had a lower penetration distance (1.00 Å) than EAC-IPA, suggesting it is not a viable extractant. Additionally, the binding energies for H-bonds and IGMH were most favorable for the ethaline−IPA complex. LLE experiments demonstrate a very good distribution coefficient of 0.46, and a selectivity of 6.45 for ethaline, indicating that this DES can efficiently separate IPA from EACs.

Motivated by the inefficiency of current fuel oil desulfurization methods, Deng et al.[39] investigated the potential of DESs for LLE of thiophenes in fuels, using DESs based on various ILs, including ChCl, combined with either EG, DEG, or MEA as HBD. They experimentally tested DES-HBD mixtures in 1:1, 1:2, and 1:4 molar ratios of HBAs to HBDs, with varying temperatures and concentrations of dibenzothiophene (DBT) in a model oil (*n*-heptane). ChCl: DEG (1:4) was identified as the optimal DES for desulfurization. QC calculations and MD simulations were conducted to rationalize the results. QC calculations were employed to optimize the geometry of the DES-HBDs and obtain the σ-profiles. These profiles revealed

https://doi.org/10.1021/acs.jced.4c00505
J. Chem. Eng. Data 2025, 70, 19−43

that for each DES, the complexes with MEA, EG, and DEG differ in both the HBD and HBA regions. The results showed that ChCl-DEG is the most effective HBD for interacting with DBT in extractive desulfurization.

MD simulations of the DES-DEG systems were carried out to investigate the mechanisms of extractive desulfurization. RDFs characterized the interaction between DBT and the solvent components, showing that DEG in the ChCl-DEG system has a strong interaction and is in close proximity to DBT, highlighting its effectiveness in surrounding DBT for desulfurization. SDFs provided a 3D view of the molecular arrangement, revealing a high density of DEG molecules around DBT, which correlated to the stronger extraction efficiency of this cosolvent. The calculated diffusion coefficient further supported stronger DES-DBT interactions for the ChCl/DEG system.

Similarly, the recent work from Wu et al.[38] focuses on developing an appropriate solvent for extracting phenols from oil mixtures. They considered combinations of ChCl with four glycols (EG, DEG, TEG, and TTEG). These mixtures were prepared and tested for their phenol-extracting capabilities using a model oil consisting of phenol and toluene. ChCl-EG was experimentally observed to be the most effective for phenol extraction, achieving an extraction efficiency of 94.02%, while incorporating the least amount of toluene at 0.449 g. The extraction efficiency decreased as the chain length of the HBDs increased: ChCl-DEG > ChCl-TEG > ChCl-TTEG.

DFT calculations and MD simulations were conducted to further explore these findings. The σ-profiles (see Figure 9) were calculated to identify the intermolecular interactions within the mixtures, providing insight into why the DES containing EG exhibits the least toluene incorporation, whereas TTEG leads to a greater incorporation of toluene.

DFT calculations at the B3LYP/6-311+G(d,p) level were performed on the individual components and their complexes to identify regions where stronger H-bonds can form. This analysis involved examining MEPs, intermolecular penetration diagrams, nonbonded interaction energies, and IGMH, which showed that increasing the glycol chain length reduces selectivity toward phenol. The analysis highlighted that the ionic liquid primarily engages in H-bonding interactions with phenol with stronger interactions between the OH group of phenol and Cl^-. MD simulations were performed to gain better insights into the average interactions among the mixture's components. The DESs simulated included those with the shortest and longest glycols (EG and TTEG). Analysis of the nonbonded interactions indicated that DESs with EG have stronger interactions with phenol than with toluene, whereas the DES with TTEG exhibited higher interaction energy with toluene. Analysis of the RDF and SDF functions underscored the predominant role of Cl^- in binding with phenol. The calculated diffusion coefficients further indicated stronger interactions within the DES containing EG compared to TTEG.

3.3. Creation of Ternary and Quaternary DES. The mixture of DESs in specific proportions with a third NATC (which can also be a solid rather than a liquid solvent) can generate ternary DES (TDES), resulting in a lower melting point than each of the individual components and enhanced capabilities for specific tasks or improved properties, such as increased stability by reducing component separation when interacting strongly with a solute.

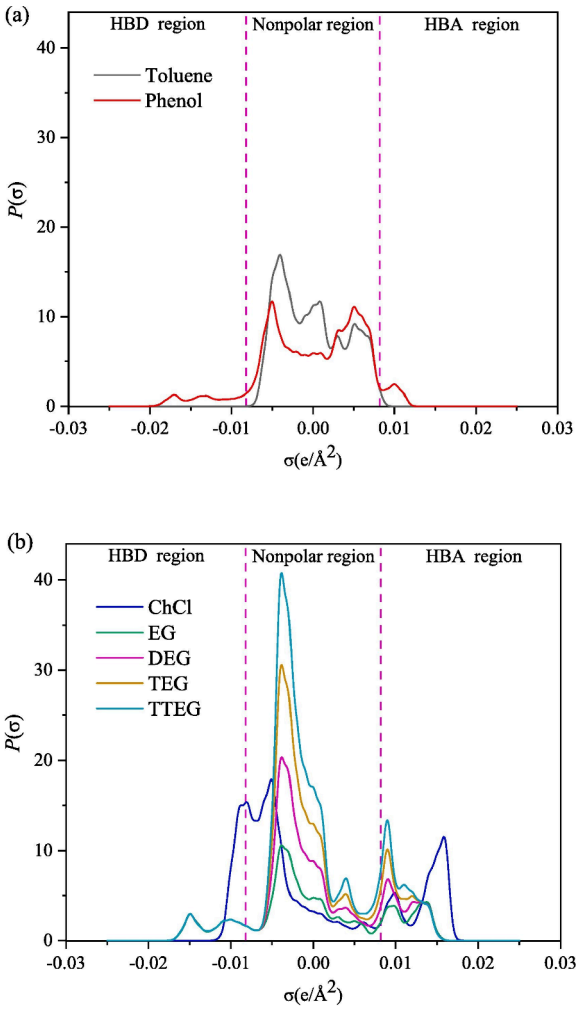

Figure 9. σ-profiles of (a) Toluene, Phenol; (b) ChCl, EG, DEG, TEG, and TTEG. Reprinted with permission from ref 38. Copyright 2024 Elsevier.

It is important to note that similar to the term DES, the term TDES is often used to describe a mixture with a specific stoichiometric ratio of components, even if it does not necessarily correspond to a deep eutectic point. Computational tools are being increasingly used to understand how the additional components affect the structure of DES and improve the properties of interest.

In their pursuit of developing efficient, stable, and environmentally friendly materials for NH_3 absorption, Li et al.[42] designed a new hybrid DES, specifically a ternary mixture (TDES) composed of ChCl/resorcinol/glycerol in a 1:3:5 ratio. It is notable for its flexible supramolecular H-bonded network, which enables strong NH_3−DES interactions while maintaining the stability of the supramolecular structure, even in the presence of such strong interactions with NH_3. The authors employed a combination of NMR spectroscopy and MD simulations to investigate the H-bonded molecular structure of TDES and its interactions with NH_3, aiming to understand its remarkable NH_3 uptake performance. MD simulations confirmed the existence of a complex H-bonded supramolecular network in the DES, with strong H-bonds existing between chloride and the hydroxyl hydrogen atoms of all DES components (Cl−H and O−H RDFs). The important role of glycerol in forming this H-bonded network was

https://doi.org/10.1021/acs.jced.4c00505
J. Chem. Eng. Data 2025, 70, 19−43

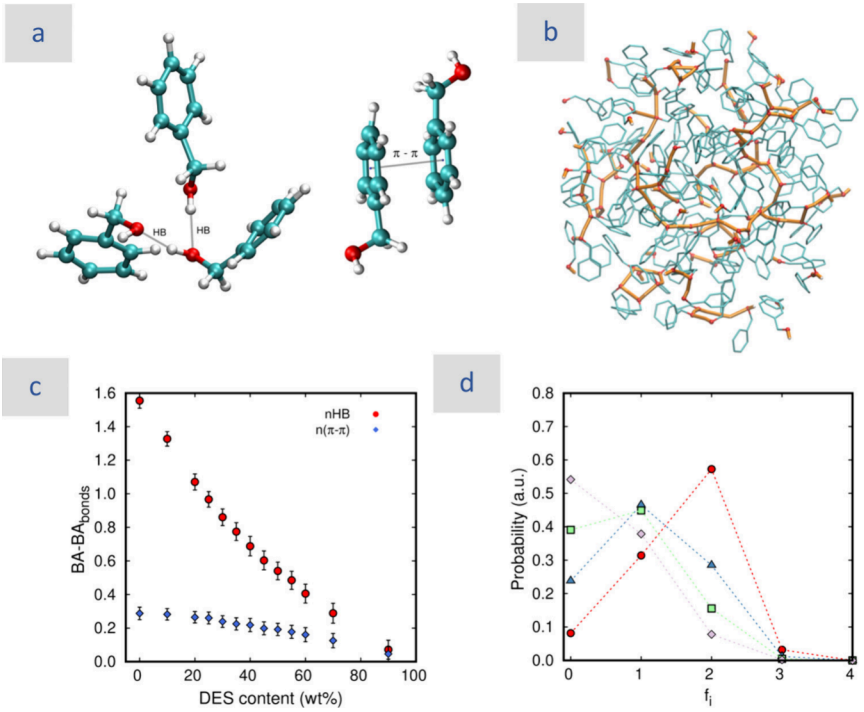

Figure 10. (a) MD simulation configurations showing BA self-interaction modes. (b) Representation of the H-bonded network in an MD simulation of pure BA; H-bonds are colored orange. (c) Average number of H-bonds, nHB, and $\pi-\pi$ interactions, n($\pi-\pi$), per BA molecule in simulated TDES + BA mixtures. (d) Probability of BA molecules engaging in H-bonds for TDES:BA molar ratios of 1:0 (circles), 1:5.4 (triangles), 1:11 (squares), and 1:22 (diamonds). Reprinted with permission from ref 33. Copyright 2020 American Chemical Society. The authors conclude that BA allows for a significantly higher TDES dilution (60−67 wt % BA) while maintaining TDES properties than that found for the corresponding TDES + water mixtures at 18−20 wt % TDES.[32] This difference is not ascribed to stronger interactions between the TDES and BA vs water but instead to the higher solubility of individual TDES components in BA.

highlighted. The simulations further showed that, following NH_3 absorption, all DES hydroxyl groups engage in H-bonds with the ammonia nitrogen atom but that the chloride anion solvation shell remains undisturbed. These findings were supported by 1H NMR chemical shift analysis. The authors conclude that the interactions between the DES components are not significantly affected by the introduction of NH_3, which accounts for the experimentally observed stability of the DES following NH_3 absorption.

Lopez-Salas et al.[32] studied the liquid structure and dynamics of the ChCl/resorcinol/urea 1:3:2 TDES adding water as a fourth component of the mixture. They studied this "water-in-TDES" mixture using a combination of neutron diffraction with isotopic substitution (NDIS), NMR- and Brillouin spectroscopies, and MD simulations. The authors showed that aqueous dilutions of the TDES in the high-dilution range of the "water-in-DES" regime results in a new *quaternary* eutectic with an even lower melting point and much lower viscosity than the pure TDES, with water acting as additional HBD or HBA. RDFs and coordination numbers obtained from NDIS through the empirical potential structure refinement (EPSR) procedure agreed well with those computed from MD simulations and showed that, in the pure TDES, resorcinol acts as a second HBD, HBA and it also self-associates within the H-bond network formed by the other TDES components. Strong interactions among the other TDES components are not significantly disrupted by the inclusion of resorcinol. Chloride anion coordination numbers (from NDIS-EPSR and MD) and diffusion coefficients (MD) reveal two well-differentiated linear regimes as a function of water content, corresponding to "water-in-DES" and "DES-in-water", and the transition compositions obtained by experiment and simulation are in good agreement at ca. 18−20 wt % water. In the following paper, Lopez-Salas et al.[33] replaced water with BA, an organic solvent capable of forming H-bonds. NDIS-ESPR-derived coordination numbers for the chloride anion and BA reveal that BA is successfully incorporated into the TDES structure up to TDES:BA 1:11 molar ratio, i.e., TDES content only 33 wt %. Brillouin, 1H NMR (chemical shifts, self-diffusion coefficients, and relaxation times), and MD simulations (self-diffusion, coordination numbers) confirm the "BA-in-DES" to "DES-in-BA" transition in the dilution range 33−40 wt % TDES. The MD simulations also provided information on the nature of BA self-interactions (Figure 10) that assisted in delineating the two dilution regimes.

3.4. Structure and Interactions. Most of the modeling studies discussed in this Perspective focus on understanding the key interactions that occur at the molecular level within these complex systems. Understanding aggregation and nanoscale phase separation phenomena in such mixtures is important for tailoring DESs systems for a variety of applications and to rationalize and predicting macroscopic properties. The most common applications for DES + NATC are for LLE, and those studies focused on this subject are treated in a dedicated section.

One of the first studies using molecular modeling to investigate the structural properties of DES + NATC systems was presented in 2016 by Harifi-Mood et al.[30] They aimed to determine whether solvatochromic probes could be used to understand the physicochemical properties, of DES + DMSO

https://doi.org/10.1021/acs.jced.4c00505
J. Chem. Eng. Data 2025, 70, 19−43

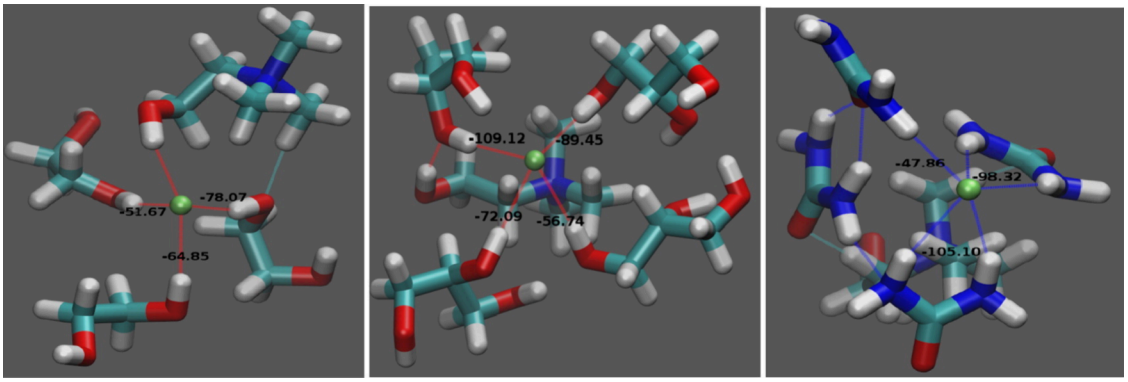

Figure 11. Simulation snapshots of chloride coordination shells in (left) ethaline, (center) glyceline, and (right) reline, optimized at the B3LYP/6-31G theory level, in the gas phase. The interaction energies of each component with the anion are shown next to the red line representing a H-bond (units of kJ/mol). Reprinted with permission from ref 30. Copyright 2016 Elsevier.

mixtures by studying the solvation of 4-nitroanisole and 4-nitroaniline in mixtures of reline, ethaline, and glyceline with DMSO. Solvatochromic probes reveal insights into the surrounding solvent environment through changes in their color or spectral properties, which can be used to compute solvatochromic parameters and provide information about intermolecular interactions. MD simulations and QM calculations were conducted to understand the solvation structures of these probes. An examination of the UV−vis absorption spectra for the solvatochromic probes 4-nitroanisole and 4-nitroaniline demonstrated that incorporating DMSO into DESs caused a reduction in polarity and HBD capacity while increasing HBA capability. Furthermore, it was observed that the probes were preferentially solvated by DMSO. MD simulations corroborated these findings, showing that the number of H-bonds involving the probe molecules in the DES mixtures diminished as the DMSO concentration increased. The researchers then concentrated on the interactions within the DESs, calculating the average Cl-DES HBD interaction energies directly from MD simulations, as well as from representative configurations extracted from MD trajectories and refined at the B3LYP/6-31G level (Figure 11). These calculations underscored the significant influence of the H-bond interactions in shaping the properties of DESs, with the Cl-HBD interaction strengths ranked in the order of ethylene glycol < glycerol < urea.

The authors later extended their solvatochromic probe-based methodology to study mixtures of the DESs reline, ethaline, and glyceline with PEG 400, a low-weight polyethylene oligomer constituted by approximately 8−9 condensed ethylene moieties.[31] MD simulations showed that PEG 400 engages in strong H-bonding interactions with the DESs and facilitates their interaction with the more hydrophobic solvatochromic probe molecules. RDFs, coordination numbers, and H-bond analyses computed from the simulations further confirm the experimentally found preferential solvation of the probe molecules by PEG 400. TD-DFT was used to predict the maximum UV absorption wavelengths of molecular clusters and corroborated experimental absorption trends, confirming that the probes are preferentially solvated by PEG 400 in these mixtures. Concerning the effect of PEG 400 on the DES structure, the authors noted that choline tends to interact with chloride via its hydroxyl group, forming H-bonds that are slightly stronger than those with other DES components. The intermolecular interactions in reline + DMSO mixtures using MD simulations were further investigated by Shah et al.[29] and compared with previous results on reline/water mixtures. RDFs and H-bond analysis revealed that DMSO preserves the characteristic reline intermolecular interactions, specifically interionic interactions, better than water: the choline−chloride H-bonded interactions do not change significantly with an increase in DMSO content. DMSO interacts more strongly with urea than ionic DES components, whereas water interacts primarily with the chloride anion. An interaction energy analysis showed that urea−urea interactions are particularly favorable in reline + DMSO mixtures.

D'Angelo, Busato, and co-workers used a combined experimental and computational approach to study how different cosolvents affect the structure of DES. They explored both polar cosolvent capable of forming H-bonds, such as MeOH[40] and apolar cosolvents that do not participate in H-bonding networks, such as *n*-hexane,[41] can affect the DES structure. They also highlighted the differences between water and methanol as cosolvents.[107] These studies are detailed in the following.

Busato et al. initially studied the DES formed by ChCl + sesamol (1:3) alone,[108] a low-transition temperature DES (see the components in Figure 12) with potential for liquid−liquid

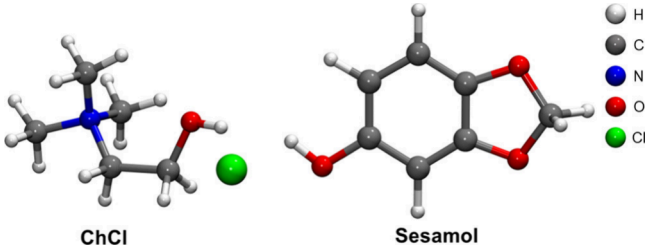

Figure 12. ChCl + sesamol 1:3 DES components: ChCl (left), and sesamol (right). Reprinted with permission from ref 40. Copyright 2021 American Chemical Society.

microextraction applications, and then its mixtures with MeOH, a cosolvent that can reduce the viscosity to better perform as extractant.[40] To this end, they performed a combined experimental and MD simulation study, investigating the intermolecular interactions and nanoscale liquid structure of mixtures of this "quasi-hydrophobic" ChCl + sesamol (1:3) DES-MeOH mixture. SWAXS experiments revealed that no nanoscale phase separation or inhomogene-

https://doi.org/10.1021/acs.jced.4c00505
J. Chem. Eng. Data 2025, 70, 19−43

ities occur in these mixtures, unlike in aqueous mixtures of this DES, where pseudophase segregation was observed.[107]

Atomistic MD simulations corroborated the authors' SWAXS analysis and provided additional molecular-level information through the calculation of Cl-hydroxyl hydrogen RDFs and coordination numbers. They found that MeOH molecules readily displace choline cations and sesamol from the chloride solvation shell (Figure 13), but this does not promote the interaction among these displaced species or their self-association. Instead, these DES components interact with excess MeOH molecules. MeOH molecules also form H-bonds among themselves. The authors conclude that methanol's ability to interact favorably with all components of the mixture underpins its formation of phase-homogeneous DES mixtures. Furthermore, the structural information obtained can aid in identifying suitable target species and conditions for its extraction applications.

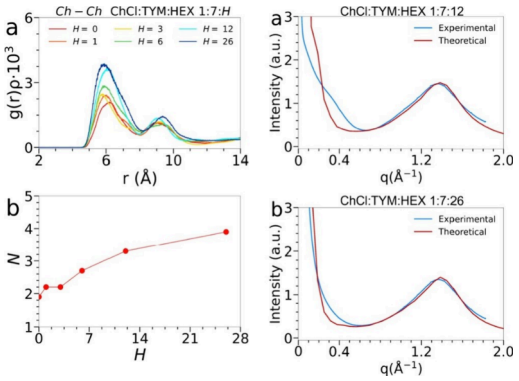

Figure 13. Comparison of experimental and MD-derived SWAXS patterns: Left (a) ChCl/thymol/hexane 1:7:12; Left (b) ChCl/thymol/hexane 1:7:26. Right (a) Choline-choline center-of-mass RDFs at different ChCl/thymol/hexane 1:7:*H* molar ratios. Right (b) Corresponding coordination numbers, *N*, obtained by integration of RDFs to first minimum, as a function of *H*; note the increase in *N* with increasing DES dilution, indicating increasing choline aggregation in pseudophase. Adapted with permission from ref 41. Copyright 2024 Elsevier.

In a recent investigation, Busato and co-workers extended their combined SWAXS-MD methodology to study the effect of *n*-hexane on the molecular to nanoscale structures of DESs of increasing hydrophobicity: ChCl + thymol 1:7 (least hydrophobic) and two Type V DESs (composed entirely of neutral species and more hydrophobic).[41] SWAXS suggested the presence of nanoscale inhomogeneities for mixtures of the ChCl + thymol DES with *n*-hexane, while the Type V DESs were found to form uniform mixtures. MD simulations yielded SWAXS patterns that were in good agreement with experiment (Figure 14), and revealed that, even though *n*-hexane interacts favorably with thymol in the ChCl/thymol/*n*-hexane system, its low affinity for the ionic DES component (ChCl) is the driving force for nanoscale and, at high hexane concentrations, macroscopic phase separation. The formation of such inhomogeneities is reflected in choline−choline center-of-mass RDFs and the corresponding coordination numbers in Figure 14. The authors conclude that DES hydrophobicity is key to understanding the nanostructures of DES + apolar cosolvent mixtures, which has important implications for all applications in which DESs are diluted with such cosolvents.

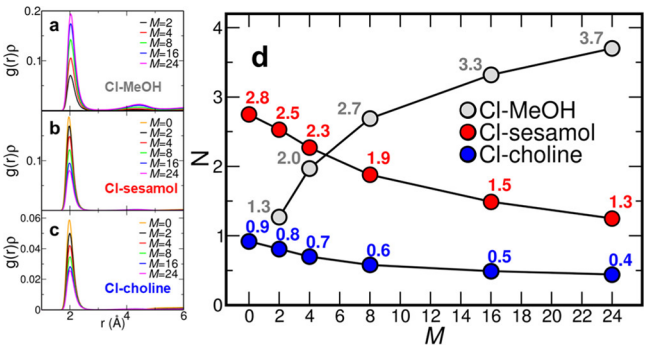

Figure 14. (Left) RDFs describing H-bonding interactions with the chloride anion in ChCl/sesamol/MeOH 1:3:*M* mixtures. Chloride-hydroxyl hydrogen RDFs for species (a) MeOH, (b) sesamol, and (c) the choline cation. (d) Coordination numbers (N) obtained by integration of RDFs in (a)−(c) up to the first minimum. Reprinted with permission from ref 40. Copyright 2021 American Chemical Society.

Kalhor et al.[36] investigated the effect on the structural organization of ethaline due to the addition of acetonitrile (ACN) using DFT methods and ATR-FTIR techniques. The "wet" experiments covered the entire concentration range of the pseudobinary mixture ethaline and ACN, while the computational study was conducted on clusters of the involved molecules, as shown in Figure 15. The geometries of the clusters were optimized starting from initial guesses guided by the complementarity of electron-rich and electron-poor regions, considering a total of 60 possible complexes.

Several properties were calculated for the optimized complexes, and the experimental ATR-FTIR peaks, combined with computational interpretations, facilitated the analysis of these peaks and the validation of the DFT data regarding the nature and strength of the interactions among the components in the mixture. The electron density at the BCPs and the Laplacian of electron density were used to investigate the H-bonds, with higher electron density values indicating stronger bonding interactions. NPA analysis using the NBO approach showed that ACN molecules increase the charge transfer from Cl^- to EG molecules, which may weaken the overall molecular interactions and likely contribute to the system's low melting point.

In a subsequent study, Kalhor et al. extended their computational approach to examine the interactions between ethaline and dimethylformamide (DMF). Using the B3LYP/6-311++G(d, p) level of theory, various clusters of ethaline−DMF were optimized and the interactions between the components were analyzed in terms of NPA, vibrational spectra, reduced density gradient, and frontier molecular orbitals. The H-bond between ethaline and DMF was found to be noncovalent. DMF was unable to disrupt the Coulombic interactions or the H-bonds between Ch^+ and Cl^- or EG. NPA and vibrational analysis indicated that the charge transfer from Cl^- ions in complexes with ethaline or ethaline−DMF weakens the Cl^-−Ch^+ bond, while noncovalent bonds between EG and DMF are strengthened. The analysis was supported by experimental data from the literature.

Kumar et al.[26] performed classical MD simulations to study the effect of methanol and ethanol on reline's molecular-scale structure and dynamics. Good agreement between simulated and experimental densities was observed, except at higher alcohol concentrations, prompting a future investigation of the

https://doi.org/10.1021/acs.jced.4c00505
J. Chem. Eng. Data 2025, 70, 19−43

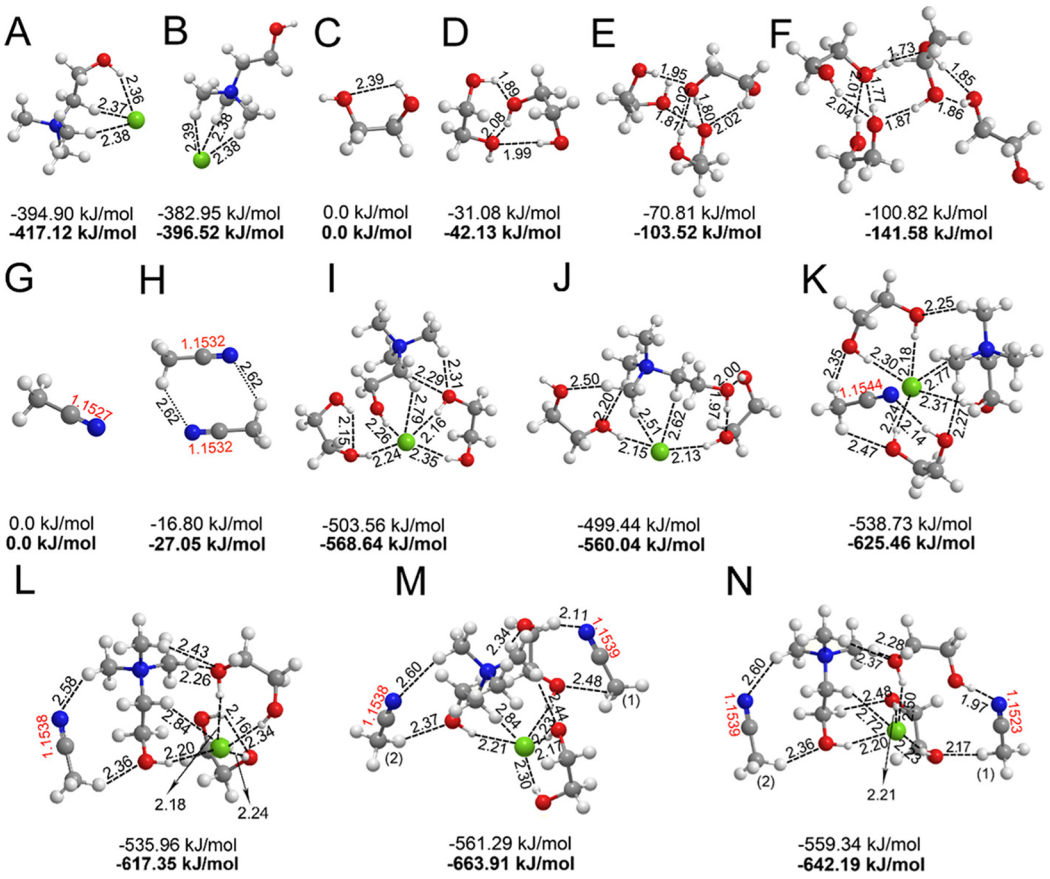

Figure 15. Optimized geometries of monomer and cluster in ethaline-ACN mixtures; distances are in Å. A, B: ChCl, C−F: monomer and clusters of EG; G-H: ACN monomer and dimer; I, J: ethaline, K−N ethaline complexes with one or two ACN molecules. For each complex, the interaction energies are reported, calculated at the B3LYP/6-311++G(d,p) level of theory and, in bold, at the M06-2X/6-311++G(d,p) level. Reprinted with permission from ref 36. Copyright 2020 American Chemical Society.

effect of nonbonded interaction mixing rules on predicting this property. A structural investigation based on RDFs, coordination numbers, and SDFs (e.g., Figure 16) was presented, showing that both alcohols interact strongly with the chloride anion through H-bonding interactions.

Panda et al.[43] investigated the microscopic structure and dynamics of the tetrabutylammonium chloride (TBAC) + ethylene glycol 1:3 DES in mixtures with either methanol or acetonitrile and compared these to previously published results for the corresponding aqueous mixtures. RDFs and electrostatic interaction energies indicated a DES-cosolvent interaction strength order: water > methanol > acetonitrile. This order correlates with the cosolvent polarity and the presence of acidic hydrogen atoms. Unlike aprotic acetonitrile, methanol interacts strongly with the DES chloride anion. Scattering patterns computed from the MD simulations suggest that cosolvent addition affects long-range structural correlations in the DES. Cosolvent addition also increases the mobility of DES components, with the increase being greater for DES + acetonitrile due to the lower number of H-bonds. The microviscosity of the DES components and cosolvent decreases with increasing cosolvent concentration, as judged by the computed rotational correlation times.

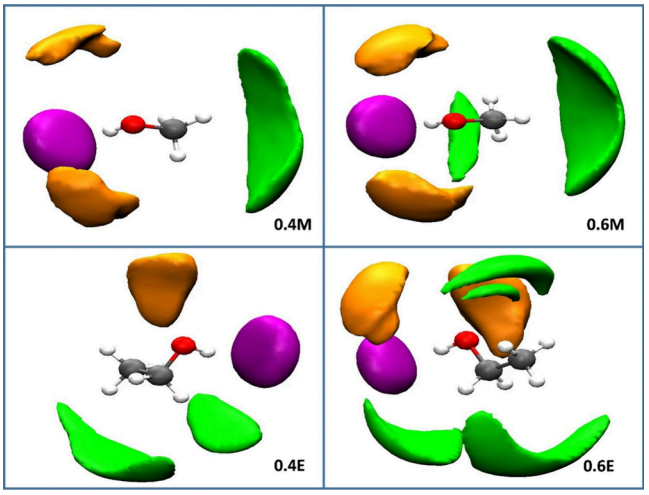

Figure 16. SDFs of DES components around (top) methanol and (bottom) ethanol cosolvents at two cosolvent mole fractions: (left) 0.4, and (right) 0.6. SDF color code: purple, chloride anion; green, urea; orange, choline cation. The SDF isovalues are 22.07 for chloride, 9.44 for urea, and 4.45 for choline. Reprinted with permission from ref 26. Copyright 2022 Springer Nature.

4. CONCLUSIONS

Both DES and IL systems are highly tailorable to specific properties and particular applications. Examples of these methods are catalysis, extraction, and materials synthesis. Since the hypothetical number of these systems is astronomically large by simply permuting all possible cations, anions, H-bond donors, H-bond acceptors, and cosolvents, molecular modeling and simulations will have an increasingly important

https://doi.org/10.1021/acs.jced.4c00505
J. Chem. Eng. Data 2025, 70, 19−43

role both in screening and in research and development to predict and, even pinpoint the right specific properties for new applications. In all types of applications, it is crucial to understand both the solvation dynamics and transport properties of DES, including the viscosity, conductivity, and electrochemistry for energy storage. Modeling, theory, and experiment combined will give detailed insight into optimizing these materials to be used in batteries, supercapacitors, and other electrochemical devices. Other examples are refrigerants and heat transfer fluids, 3D printing of functional materials, medical sensors due to their sensitivity and selectivity, and much more. DES will continue to contribute to green chemistry and sustainability by being environmentally friendly solvents for future chemical reactions. Biocompatible and stable DES and IL systems will be used more and more in drug delivery as drug carriers with specific release profiles of pharmaceutical formulations. Modeling and simulations will be key components in future innovative research.

There are obstacles in modeling and simulations, coming from the high complexity of DES and DES + cosolvents themselves. They exhibit a uniquely broad spectrum of short- and long-range interactions. Indeed, they interact with themselves and other types of molecules with all possible interactions in concert, and fine-tuning them becomes a highly complicated task. To study complex systems as DESs, using modeling and simulation methods requires not only a combination of different tools (as hybrid and complementary) but also methodological improvements and in particular new strategies to develop and parametrize force fields, the key input in MD simulations. These include new and robust polarizable force fields that are not expensive to use. Access to both experimental and theoretical/simulation data that can be used in parametrization aided with AI methods. Common molecular mechanical force fields (MMFF) are conceptually simple constructions of interaction potentials, where all contributions are assumed to be additive on top of each other. Parameterization of them is challenging, and even when managed, the transferability of FFs is not guaranteed. Available FFs are not initially well-parametrized for the highly complex DES and IL systems, having several unique interactions, including strong H-bonds and mutually correlated ionic interactions. Electronic polarization and charge delocalization effects cannot be easily implemented in standard force fields. It is the charge transfer in conjugated ring structures that makes calculations of partial charges tricky. Often ad hoc types of rules of thumb are applied like empirical scaling factors, which even in accurate force fields can reduce the predictive value of modeling and simulations. Due to long-range structural correlations in DES, seen in several diffraction studies and the strong heterogeneous character of DES and IL, very long simulations are required to obtain equilibrated results, so short length and time scales soon become issues. Accelerated sampling techniques are important for these heterogeneous systems containing slow and rare dynamic events. Many of the problems mentioned above could, in principle, be solved using QM modeling and simulation methods. However, with these methods the computational cost increases rapidly, leading to studies focusing on smaller systems, where the long-range complexity and heterogeneity of the DES systems are lost. Fragment-based QM methods, like COSMO-RS, have been successful for DES systems and should be used more due to their connection to solvation phenomena via thermodynamics. Also, bottom-up multiscale modeling methods from first-principles should be used to connect length and time scales more, by combining QM and atomistic simulations to coarse-grained and mesoscale models.

Additional and more principal issues concern the common practices and protocols used in modeling and simulation of DES systems with NATC. We want to take this occasion to point out several weaknesses we encountered in the papers we have reviewed and advise on how they could be corrected. We noted that very often, the molecular clusters on which certain QM properties are calculated are not properly defined, making it difficult to reproduce the computational data. For example, the optimized geometries, obtained through a minimization procedure, strongly depend on the starting geometry. The relevance of the properties calculated for a particular cluster depends on how likely that cluster is to occur in real systems. As Mullins et al. observed, "The molecular conformation used in the DFT calculation has a large effect on the σ-profile, and, therefore, great care should be taken in obtaining a low-energy geometry".[109] This consideration is crucial for all properties derived from QM calculations on a single molecule and often much more for a cluster. Proper sampling of the conformational space is essential, and publications should clearly describe how the conformational space of the clusters considered for calculating a given property has been explored. Additionally, the equilibration of MD simulations must be carefully checked to ensure that the system has reached a stable and representative state before deriving any properties. Authors and reviewers must ensure that the information required to fully reproduce a computational experiment, including details on MD equilibration, is presented in the main manuscript or supporting materials. Concerning the force field used, there is still a lack of benchmarking the different force field and parameters combination when used for these highly complex systems.

The approach of sampling the conformational space through extended MD, analyzing the clustering of relevant components, and calculating QM properties on the most relevant clusters has been used in various studies with great success.

To summarize the key findings, we can see that computational chemistry studies, in particular those with QM calculations and MD simulations, of DES mixtures with cosolvents, other than water, show clearly their important role in

- giving both a broader and deeper understanding of the diverse molecular interactions in complex liquid systems
- giving detailed knowledge of the highly heterogeneous structure with long-range correlations.
- showing how even small amounts of cosolvent can change the landscape of interactions, structure, thermodynamics and dynamics
- guiding studies to tailor the multifaceted and delicate properties for applications in great variety of fields from adsorption of gases to extraction of selected components from complex mixtures
- understanding and tuning transport properties: diffusion, viscosity, conductivity (heat and electric) for emerging applications
- contributing to new knowledge of how to improve both solubility and reactivity by choosing a cosolvent.

Based on these findings that highlight the usefulness of computational tools and considering the increasing access to computational resources and free software, we believe that this

https://doi.org/10.1021/acs.jced.4c00505
J. Chem. Eng. Data 2025, 70, 19−43

approach will become more important, not only for understanding the complex organization of these solvents, but also for the computationally guided design of efficient solvents for applications such as extraction and viscosity reduction. In addition, we believe that the computational tools will be increasingly used as the availability of computing resources increases, both in terms of hardware and available software, and with increasing interest in the applications of DES + cosolvent mixtures, the computational approach is going to be more and more used—not only by molecular modeling specialists, but also by experimentalists groups. In this context, it is important to provide a few guidelines for the future developments:

- for QM calculations, before calculating the properties of interest, 1) evaluate carefully the conformational space accessible to the studied molecules, and how it could be affected by aggregation in the condensed phase; 2) when possible, perform classical MD simulations to sample the conformational space, and verify how much the QM properties of interest depend on the chosen configuration and on how many configurations are required to reach a converged value; 3) include the coordinates of the systems modeled in the Supporting Information for reproducibility; 4) include the details required for reproducing the calculations in the Supporting Information.
- for FF based molecular simulations, it is fundamental to always consider that they are based on strong approximations, and the results cannot be considered as valid without: 1) carefully verifying the performance of the force field on similar systems present in literature; 2) carefully evaluating that the system has reached the equilibrium state before selecting the portion of the trajectory to be analyzed and clearly comment this point in the manuscript or Supporting Information; and 3) when possible, evaluate the quality of the simulations against some experimental observable (most simple being the density and the diffusion constant) as seen in some of the articles reviewed here; 4) if feasible, compare the performance of different force fields, especially when no experimental evidence can be used to validate the results; and 5) since the results of the simulations depends on the FF used for each componenents and on the setting of the simulations, all the details of the simulations (number of particles, algorithms used to keep pressure or temperature constant, time steps, etc.) should be reported in the papers or in the Supporting Information.

■ ASSOCIATED CONTENT

Special Issue Paper

This paper was intended for the In Honor of Xiaohua Lu special issue, published as the December 2024 issue of *J. Chem. Eng. Data* (Vol. 69, No. 12).

■ AUTHOR INFORMATION

Corresponding Authors

Xiaoyan Ji − *Division of Energy Science, Energy Engineering, Luleå University of Technology, 97187 Luleå, Sweden;* orcid.org/0000-0002-0200-9960; Email: xiaoyan.ji@ltu.se

Aatto Laaksonen − *Division of Energy Science, Energy Engineering, Luleå University of Technology, 97187 Luleå, Sweden; Centre of Advanced Research in Bionanoconjugates and Biopolymers, "Petru Poni" Institute of Macromolecular Chemistry, 700487 Iasi, Romania; Division of Physical Chemistry, Arrhenius Laboratory, Department of Materials and Environmental Chemistry, Stockholm University, 10691 Stockholm, Sweden; State Key Laboratory of Materials-Oriented and Chemical Engineering, Nanjing Tech University, 210009 Nanjing, China;* orcid.org/0000-0001-9783-4535; Email: aatto@mmk.su.se

Francesca Mocci − *Department of Chemical and Geological Sciences, University of Cagliari, 09042 Monserrato, Italy;* orcid.org/0000-0003-1394-9146; Email: fmocci@unica.it

Authors

Leon de Villiers Engelbrecht − *Division of Energy Science, Energy Engineering, Luleå University of Technology, 97187 Luleå, Sweden;* orcid.org/0009-0000-2690-6079

Narcis Cibotariu − *Centre of Advanced Research in Bionanoconjugates and Biopolymers, "Petru Poni" Institute of Macromolecular Chemistry, 700487 Iasi, Romania;* orcid.org/0009-0001-7932-7983

Complete contact information is available at: https://pubs.acs.org/10.1021/acs.jced.4c00505

Author Contributions

#L.d.V.E. and N.C. contributed equally to this work.

Notes

The authors declare no competing financial interest.

■ ACKNOWLEDGMENTS

Dedicated to Professor Xiaohua Lu in celebration of his 65th birthday, in recognition of his outstanding contributions to the field of Molecular Thermodynamics, with gratitude for his inspiration to generations of scholars. A.L. and N.C. acknowledge financial support from European Union's Horizon Europe Research and Innovation Programme under grant agreement No 101086667, project BioMat4CAST (BioMat4CAST - "Petru Poni" Institute of Macromolecular Chemistry Multi-Scale in Silico Laboratory for Complex and Smart Biomaterials). L.E. acknowledges financial support from the Kempe Foundation (Project: SMK21-0011). X.J. acknowledges financial support from Horizon-EIC, Pathfinder challenges, Grant Number: 101070976. All the authors acknowledge the COSY COST ACTION CA21101.

■ REFERENCES

(1) Hansen, B. B.; Spittle, S.; Chen, B.; Poe, D.; Zhang, Y.; Klein, J. M.; Horton, A.; Adhikari, L.; Zelovich, T.; Doherty, B. W.; Gurkan, B.; Maginn, E. J.; Ragauskas, A.; Dadmun, M.; Zawodzinski, T. A.; Baker, G. A.; Tuckerman, M. E.; Savinell, R. F.; Sangoro, J. R. Deep Eutectic Solvents: A Review of Fundamentals and Applications. *Chem. Rev.* **2021**, *121* (3), 1232−1285.

(2) De Sloovere, D.; Vanpoucke, D. E. P.; Paulus, A.; Joos, B.; Calvi, L.; Vranken, T.; Reekmans, G.; Adriaensens, P.; Eshraghi, N.; Mahmoud, A.; Boschini, F.; Safari, M.; Van Bael, M. K.; Hardy, A. Deep Eutectic Solvents as Nonflammable Electrolytes for Durable Sodium-Ion Batteries. *Adv. Energy Sustain. Res.* **2022**, *3* (3), 2100159.

(3) Abbott, A. P.; Capper, G.; Davies, D. L.; Rasheed, R. K.; Tambyrajah, V. Novel Solvent Properties of Choline Chloride/Urea mixtures. *Chem. Commun.* **2003**, No. 1, 70−71.

(4) Afonso, J.; Mezzetta, A.; Marrucho, I. M.; Guazzelli, L. History Repeats Itself Again: Will the Mistakes of the Past for ILs Be Repeated for DESs? From Being Considered Ionic Liquids to Becoming Their Alternative: The Unbalanced Turn of Deep Eutectic Solvents. *Green Chem.* **2023**, *25* (1), 59−105.
(5) Buchner, R.; Agieienko, V. Ethaline and Related Systems: May Be Not "Deep" Eutectics but Clearly Interesting Ionic Liquids. *Pure Appl. Chem.* **2023**, *95* (7), 833−840.
(6) Hayler, H. J.; Perkin, S. The Eutectic Point in Choline Chloride and Ethylene Glycol Mixtures. *Chem. Commun.* **2022**, *58* (91), 12728−12731.
(7) Cappelluti, F.; Mariani, A.; Bonomo, M.; Damin, A.; Bencivenni, L.; Passerini, S.; Carbone, M.; Gontrani, L. Stepping Away from Serendipity in Deep Eutectic Solvent Formation: Prediction from Precursors Ratio. *J. Mol. Liq.* **2022**, *367*, 120443.
(8) Smith, E. L.; Abbott, A. P.; Ryder, K. S. Deep Eutectic Solvents (DESs) and Their Applications. *Chem. Rev.* **2014**, *114* (21), 11060−11082.
(9) Abranches, D. O.; Martins, M. A. R.; Silva, L. P.; Schaeffer, N.; Pinho, S. P.; Coutinho, J. A. P. Phenolic Hydrogen Bond Donors in the Formation of Non-Ionic Deep Eutectic Solvents: The Quest for Type V DES. *Chem. Commun.* **2019**, *55* (69), 10253−10256.
(10) Velez, C.; Acevedo, O. Simulation of Deep Eutectic Solvents: Progress to Promises. *WIREs Comput. Mol. Sci.* **2022**, *12* (4), No. e1598.
(11) Ma, C.; Laaksonen, A.; Liu, C.; Lu, X.; Ji, X. The Peculiar Effect of Water on Ionic Liquids and Deep Eutectic Solvents. *Chem. Soc. Rev.* **2018**, *47* (23), 8685−8720.
(12) Mariani, A.; Caminiti, R.; Ramondo, F.; Salvitti, G.; Mocci, F.; Gontrani, L. Inhomogeneity in Ethylammonium Nitrate-Acetonitrile Binary Mixtures: The Highest "Low *q* Excess" Reported to Date. *J. Phys. Chem. Lett.* **2017**, *8* (15), 3512−3522.
(13) Wang, Y.-L.; Sarman, S.; Laaksonen, A.; Golets, M.; Mocci, F.; Lu, Z.-Y. 4. Multigranular Modeling of Ionic Liquids. In *Ionic Liquids*; Fehrmann, R., Santini, C., Eds.; De Gruyter, 2019; pp 55−100. DOI: 10.1515/9783110583632-004.
(14) Alizadeh, V.; Malberg, F.; Pádua, A. A. H.; Kirchner, B. Are There Magic Compositions in Deep Eutectic Solvents? Effects of Composition and Water Content in Choline Chloride/Ethylene Glycol from Ab Initio Molecular Dynamics. *J. Phys. Chem. B* **2020**, *124* (34), 7433−7443.
(15) Mariani, A.; Engelbrecht, L.; Le Donne, A.; Mocci, F.; Bodo, E.; Passerini, S. Disclosing the Hierarchical Structure of Ionic Liquid Mixtures by Multiscale Computational Methods. In *Theoretical and Computational Approaches to Predicting Ionic Liquid Properties*; Elsevier, 2021; pp 1−67. DOI: 10.1016/B978-0-12-820280-7.00014-0.
(16) Lengvinaite, D.; Kvedaraviciute, S.; Bielskute, S.; Klimavicius, V.; Balevicius, V.; Mocci, F.; Laaksonen, A.; Aidas, K. Structural Features of the [C4mim][Cl] Ionic Liquid and Its Mixtures with Water: Insight from a ^{1}H NMR Experimental and QM/MD Study. *J. Phys. Chem. B* **2021**, *125* (48), 13255−13266.
(17) Kaur, S.; Kumari, M.; Kashyap, H. K. Microstructure of Deep Eutectic Solvents: Current Understanding and Challenges. *J. Phys. Chem. B* **2020**, *124* (47), 10601−10616.
(18) Tolmachev, D.; Lukasheva, N.; Ramazanov, R.; Nazarychev, V.; Borzdun, N.; Volgin, I.; Andreeva, M.; Glova, A.; Melnikova, S.; Dobrovskiy, A.; Silber, S. A.; Larin, S.; De Souza, R. M.; Ribeiro, M. C. C.; Lyulin, S.; Karttunen, M. Computer Simulations of Deep Eutectic Solvents: Challenges, Solutions, and Perspectives. *Int. J. Mol. Sci.* **2022**, *23* (2), 645.
(19) Wang, H.; Zuo, Z.; Lu, L.; Laaksonen, A.; Wang, Y.; Lu, X.; Ji, X. Experimental and Theoretical Study on Ion Association in [Hmim][Halide] + Water/Isopropanol Mixtures. *Fluid Phase Equilib.* **2023**, *566*, 113680.
(20) Wang, Y.; Ma, C.; Liu, C.; Lu, X.; Feng, X.; Ji, X. Thermodynamic Study of Choline Chloride-Based Deep Eutectic Solvents with Water and Methanol. *J. Chem. Eng. Data* **2020**, *65* (5), 2446−2457.
(21) Zuo, Z.; Cao, B.; Wang, Y.; Ma, C.; Lu, X.; Ji, X. Thermodynamic Study of Choline Chloride-Based Deep Eutectic Solvents with Dimethyl Sulfoxide and Isopropanol. *J. Mol. Liq.* **2024**, *394*, 123731.
(22) Zhang, Z.; Liu, X.; Yao, D.; Ma, Z.; Zhao, J.; Zhang, W.; Cui, P.; Ma, Y.; Zhu, Z.; Wang, Y. Molecular Kinetic Extraction Mechanism Analysis of 1-Butanol from n-Heptane-1-Butanol by Choline-Based DESs as Extractants. *J. Mol. Liq.* **2021**, *322*, 114665.
(23) Liu, X.; Xing, J.; Sun, M.; Su, Z.; Chen, Z.; Wang, Y.; Cui, P. Phase Behavior and Extraction Mechanism of Methanol-n-Hexane Separation Using Choline-Based Deep Eutectic Solvent. *J. Mol. Liq.* **2022**, *345*, 118204.
(24) Liu, X.; Li, Y.; Xing, J.; Li, Y.; Su, Z.; Qiu, X.; Chen, Z.; Wang, Y.; Cui, P. Liquid-Liquid Extraction and Mechanism Analysis of Extracting Fuel Additive Isopropanol from Mixture with Choline-Based Deep Eutectic Solvents as Efficient Extractants. *Fuel* **2022**, *326*, 125048.
(25) Dai, Y.; Chu, X.; Jiao, Y.; Li, Y.; Shan, F.; Zhao, S.; Li, G.; Lei, Z.; Cui, P.; Zhu, Z.; Wang, Y. Molecular Insights into Azeotrope Separation in the Methyl Tert-Butyl Ether Production Process Using ChCl-Based Deep Eutectic Solvents. *Chem. Eng. Sci.* **2022**, *264*, 118179.
(26) Kumar, K.; Bharti, A.; Mogurampelly, S. Insights on Choline Chloride-Based Deep Eutectic Solvent (Reline) + Primary Alcohol Mixtures: A Molecular Dynamics Simulation Study. *J. Mol. Model.* **2022**, *28* (2), 30.
(27) Dawass, N.; Langeveld, J.; Ramdin, M.; Pérez-Gallent, E.; Villanueva, A. A.; Giling, E. J. M.; Langerak, J.; Van Den Broeke, L. J. P.; Vlugt, T. J. H.; Moultos, O. A. Solubilities and Transport Properties of CO_2, Oxalic Acid, and Formic Acid in Mixed Solvents Composed of Deep Eutectic Solvents, Methanol, and Propylene Carbonate. *J. Phys. Chem. B* **2022**, *126* (19), 3572−3584.
(28) Sun, C.; Qu, Y.; Dai, Y.; Cui, P.; Wang, Y.; Zhu, Z.; Gao, J. Comparative Study on Ionic Liquids and Deep Eutectic Solvents in the Separation of Fuel Additive Isopropyl Alcohol and Ethyl Acetate by the Experimental Study and Molecular Simulation. *Fuel* **2023**, *354*, 129397.
(29) Shah, D.; Mansurov, U.; Mjalli, F. S. Intermolecular Interactions and Solvation Effects of Dimethylsulfoxide on Type III Deep Eutectic Solvents. *Phys. Chem. Chem. Phys.* **2019**, *21* (31), 17200−17208.
(30) Harifi-Mood, A. R.; Ghobadi, R.; Matić, S.; Minofar, B.; Reha, D. Solvation Analysis of Some Solvatochromic Probes in Binary Mixtures of Reline, Ethaline, and Glyceline with DMSO. *J. Mol. Liq.* **2016**, *222*, 845−853.
(31) Aryafard, M.; Abbasi, M.; Reha, D.; Harifi-Mood, A. R.; Minofar, B. Experimental and Theoretical Investigation of Solvatochromic Properties and Ion Solvation Structure in DESs of Reline, Glyceline, Ethaline and Their Mixtures with PEG 400. *J. Mol. Liq.* **2019**, *284*, 59−67.
(32) López-Salas, N.; Vicent-Luna, J. M.; Imberti, S.; Posada, E.; Roldán, M. J.; Anta, J. A.; Balestra, S. R. G.; Madero Castro, R. M.; Calero, S.; Jiménez-Riobóo, R. J.; Gutiérrez, M. C.; Ferrer, M. L.; del Monte, F. Looking at the "Water-in-Deep-Eutectic-Solvent" System: A Dilution Range for High Performance Eutectics. *ACS Sustain. Chem. Eng.* **2019**, *7* (21), 17565−17573.
(33) López-Salas, N.; Vicent-Luna, J. M.; Posada, E.; Imberti, S.; Madero-Castro, R. M.; Calero, S.; Ania, C. O.; Jiménez-Riobóo, R. J.; Gutiérrez, M. C.; Ferrer, M. L.; Del Monte, F. Further Extending the Dilution Range of the "Solvent-in-DES" Regime upon the Replacement of Water by an Organic Solvent with Hydrogen Bond Capabilities. *ACS Sustain. Chem. Eng.* **2020**, *8* (32), 12120−12131.
(34) Cea-Klapp, E.; Garrido, J. M.; Quinteros-Lama, H. Insights into the Orientation and Hydrogen Bond Influence on Thermophysical and Transport Properties in Choline-Based Deep Eutectic Solvents and Methanol. *J. Mol. Liq.* **2022**, *345*, 117019.
(35) Engelbrecht, L. D. V.; Ji, X.; Carbonaro, C. M.; Laaksonen, A.; Mocci, F. MD Simulations Explain the Excess Molar Enthalpies in

Pseudo-Binary Mixtures of a Choline Chloride-Based Deep Eutectic Solvent with Water or Methanol. *Front. Chem.* **2022**, *10*, 983281.
(36) Kalhor, P.; Xu, J.; Ashraf, H.; Cao, B.; Yu, Z.-W. Structural Properties and Hydrogen-Bonding Interactions in Binary Mixtures Containing a Deep-Eutectic Solvent and Acetonitrile. *J. Phys. Chem. B* **2020**, *124* (7), 1229−1239.
(37) Kalhor, P.; Yarivand, O.; Seifpanahi-Shabani, K. Quantum Chemical Calculations on Dissolution of Dimethylformamide in Ethaline. *J. Mol. Graph. Model.* **2021**, *107*, 107966.
(38) Wu, H.; Li, X.; Chen, Q.; Liu, Z.; Wang, X.; Zhang, W.; Miao, Y.; Yao, C. Molecular Mechanism and Extraction Performance Evaluation of Choline Chloride-Based Deep Eutectic Solvents for Phenol Separation from Oil: Different Glycols as Hydrogen Bond Donors. *Fuel* **2024**, *367*, 131530.
(39) Deng, H.; Wang, X.; Chen, J.; Zhao, J.; Jiang, Z.; Tian, Z.; Du, P.; Li, Y. Experimental and Molecular Dynamics Study of Fuel Desulfurization Process Using Deep Eutectic Solvent. *J. Environ. Chem. Eng.* **2023**, *11* (3), 110277.
(40) Busato, M.; Del Giudice, A.; Di Lisio, V.; Tomai, P.; Migliorati, V.; Gentili, A.; Martinelli, A.; D'Angelo, P. Fate of a Deep Eutectic Solvent upon Cosolvent Addition: Choline Chloride-Sesamol 1:3 Mixtures with Methanol. *ACS Sustain. Chem. Eng.* **2021**, *9* (36), 12252−12261.
(41) Mannucci, G.; Tofoni, A.; Busato, M.; D'Angelo, P. Hydrophobicity as the Key to Understanding the Nanostructural Behavior of Eutectic Mixtures upon Apolar Cosolvent Addition. *J. Mol. Liq.* **2024**, *394*, 123746.
(42) Li, Y.; Ali, M. C.; Yang, Q.; Zhang, Z.; Bao, Z.; Su, B.; Xing, H.; Ren, Q. Hybrid Deep Eutectic Solvents with Flexible Hydrogen-Bonded Supramolecular Networks for Highly Efficient Uptake of NH_3. *ChemSusChem* **2017**, *10* (17), 3368−3377.
(43) Panda, D. K.; Bhargava, B. L. Molecular Dynamics Studies of Mixtures of a Deep Eutectic Solvent and Cosolvents. *J. Comput. Biophys. Chem.* **2023**, *22* (06), 711−723.
(44) Allen, M. P.; Tildesley, D. J. *Computer Simulation of Liquids*, 2nd ed.; Oxford University PressOxford, 2017. DOI: 10.1093/oso/9780198803195.001.0001.
(45) Laaksonen, A.; Mocci, F. Section Introduction: Molecular Dynamics Simulations and Reaction Rates. In *Comprehensive Computational Chemistry*; Elsevier, 2024; pp 315−328. DOI: 10.1016/B978-0-12-821978-2.00130-6.
(46) Leach, A. R. *Molecular Modelling: Principles and Applications*, 2nd ed.; Pearson, 2001.
(47) Klamt, A. Conductor-like Screening Model for Real Solvents: A New Approach to the Quantitative Calculation of Solvation Phenomena. *J. Phys. Chem.* **1995**, *99* (7), 2224−2235.
(48) Tan, S. P.; Adidharma, H.; Radosz, M. Recent Advances and Applications of Statistical Associating Fluid Theory. *Ind. Eng. Chem. Res.* **2008**, *47* (21), 8063−8082.
(49) Sun, Y.; Dai, Z.; Shen, G.; Lu, X.; Ling, X.; Ji, X. Accelerate the Electrolyte Perturbed-Chain Statistical Associating Fluid Theory-Density Functional Theory Calculation With the Chebyshev Pseudo-Spectral Collocation Method. Part II. Spherical Geometry and Anderson Mixing. *Front. Chem.* **2022**, *9*, 801551.
(50) Sun, Y.; Lu, X.; Shen, G.; Ji, X. Accelerate the ePC-SAFT-DFT Calculation with the Chebyshev Pseudospectral Collocation Method. *Ind. Eng. Chem. Res.* **2021**, *60* (25), 9269−9285.
(51) Sun, Y.; Tang, X.; Ji, X.; Lu, X.; Ling, X. Analysis of Vapor-Liquid Interfacial Transport Resistivities with DGT-PC-SAFT Based on the General Approach. *Ind. Eng. Chem. Res.* **2022**, *61*, 16352.
(52) Zuo, Z.; Lu, X.; Ji, X. Modeling Self-Diffusion Coefficients of Ionic Liquids Using ePC-SAFT and FVT Combined with Einstein Relation. *AIChE J.* **2024**, *70* (8), No. e18468.
(53) Zuo, Z.; Lu, X.; Ji, X. Modeling Self-Diffusion Coefficient and Viscosity of Chain-like Fluids Based on ePC-SAFT. *J. Chem. Eng. Data* **2024**, *69* (2), 348−362.
(54) Aravena, P.; Cea-Klapp, E.; Gajardo-Parra, N. F.; Held, C.; Garrido, J. M.; Canales, R. I. Effect of Water and Hydrogen Bond Acceptor on the Density and Viscosity of Glycol-Based Eutectic Solvents. *J. Mol. Liq.* **2023**, *389*, 122856.
(55) Sepúlveda-Orellana, B.; Gajardo-Parra, N. F.; Do, H. T.; Pérez-Correa, J. R.; Held, C.; Sadowski, G.; Canales, R. I. Measurement and PC-SAFT Modeling of the Solubility of Gallic Acid in Aqueous Mixtures of Deep Eutectic Solvents. *J. Chem. Eng. Data* **2021**, *66* (2), 958−967.
(56) Beckmann, J. B. B.; Rauber, D.; Philippi, F.; Goloviznina, K.; Ward-Williams, J. A.; Sederman, A. J.; Mantle, M. D.; Pádua, A.; Kay, C. W. M.; Welton, T.; Gladden, L. F. Molecular Dynamics of Ionic Liquids from Fast-Field Cycling NMR and Molecular Dynamics Simulations. *J. Phys. Chem. B* **2022**, *126* (37), 7143−7158.
(57) Wang, Y.-L.; Shah, F. U.; Glavatskih, S.; Antzutkin, O. N.; Laaksonen, A. Atomistic Insight into Orthoborate-Based Ionic Liquids: Force Field Development and Evaluation. *J. Phys. Chem. B* **2014**, *118* (29), 8711−8723.
(58) Ishizuka, R.; Matubayasi, N. Self-Consistent Determination of Atomic Charges of Ionic Liquid through a Combination of Molecular Dynamics Simulation and Density Functional Theory. *J. Chem. Theory Comput.* **2016**, *12* (2), 804−811.
(59) Wang, Y.-L.; Zhu, Y.-L.; Lu, Z.-Y.; Laaksonen, A. Electrostatic Interactions in Soft Particle Systems: Mesoscale Simulations of Ionic Liquids. *Soft Matter* **2018**, *14* (21), 4252−4267.
(60) Ge, Y.; Zhu, Q.; Li, Y.; Dong, H.; Ma, J. An Electrostatic-Variable Coarse-Grained Model for Predicting Enthalpy of Vaporization, Surface Tension, Diffusivity, Conductivity, and Dielectric Constant of Aqueous Ionic Liquid. *J. Mol. Liq.* **2022**, *346*, 118230.
(61) Shayestehpour, O.; Zahn, S. Efficient Molecular Dynamics Simulations of Deep Eutectic Solvents with First-Principles Accuracy Using Machine Learning Interatomic Potentials. *J. Chem. Theory Comput* **2023**, *19*, 8732.
(62) Wang, J.; Wolf, R. M.; Caldwell, J. W.; Kollman, P. A.; Case, D. A. Development and Testing of a General Amber Force Field. *J. Comput. Chem.* **2004**, *25* (9), 1157−1174.
(63) Wang, J.; Wang, W.; Kollman, P. A.; Case, D. A. Automatic Atom Type and Bond Type Perception in Molecular Mechanical Calculations. *J. Mol. Graph. Model.* **2006**, *25* (2), 247−260.
(64) Perkins, S. L.; Painter, P.; Colina, C. M. Molecular Dynamic Simulations and Vibrational Analysis of an Ionic Liquid Analogue. *J. Phys. Chem. B* **2013**, *117* (35), 10250−10260.
(65) Perkins, S. L.; Painter, P.; Colina, C. M. Experimental and Computational Studies of Choline Chloride-Based Deep Eutectic Solvents. *J. Chem. Eng. Data* **2014**, *59* (11), 3652−3662.
(66) Dodda, L. S.; Cabeza de Vaca, I.; Tirado-Rives, J.; Jorgensen, W. L. LigParGen Web Server: An Automatic OPLS-AA Parameter Generator for Organic Ligands. *Nucleic Acids Res.* **2017**, *45* (W1), W331−W336.
(67) Dodda, L. S.; Vilseck, J. Z.; Tirado-Rives, J.; Jorgensen, W. L. 1.14*CM1A-LBCC: Localized Bond-Charge Corrected CM1A Charges for Condensed-Phase Simulations. *J. Phys. Chem. B* **2017**, *121* (15), 3864−3870.
(68) Jorgensen, W. L.; Tirado-Rives, J. Potential Energy Functions for Atomic-Level Simulations of Water and Organic and Biomolecular Systems. *Proc. Natl. Acad. Sci. U. S. A.* **2005**, *102* (19), 6665−6670.
(69) Canongia Lopes, J. N.; Pádua, A. A. H. CL&P: A Generic and Systematic Force Field for Ionic Liquids Modeling. *Theor. Chem. Acc.* **2012**, *131* (3), 1129.
(70) Doherty, B.; Acevedo, O. OPLS Force Field for Choline Chloride-Based Deep Eutectic Solvents. *J. Phys. Chem. B* **2018**, *122* (43), 9982−9993.
(71) Poger, D.; Van Gunsteren, W. F.; Mark, A. E. A New Force Field for Simulating Phosphatidylcholine Bilayers. *J. Comput. Chem.* **2010**, *31* (6), 1117−1125.
(72) Hansen, H. S.; Hünenberger, P. H. A Reoptimized GROMOS Force Field for Hexopyranose-based Carbohydrates Accounting for the Relative Free Energies of Ring Conformers, Anomers, Epimers, Hydroxymethyl Rotamers, and Glycosidic Linkage Conformers. *J. Comput. Chem.* **2011**, *32* (6), 998−1032.

(73) Schmid, N.; Eichenberger, A. P.; Choutko, A.; Riniker, S.; Winger, M.; Mark, A. E.; Van Gunsteren, W. F. Definition and Testing of the GROMOS Force-Field Versions 54A7 and 54B7. *Eur. Biophys. J.* **2011**, *40* (7), 843−856.
(74) Abraham, M. J.; Murtola, T.; Schulz, R.; Páll, S.; Smith, J. C.; Hess, B.; Lindahl, E. GROMACS: High Performance Molecular Simulations through Multi-Level Parallelism from Laptops to Supercomputers. *SoftwareX* **2015**, *1−2*, 19−25.
(75) Salomon-Ferrer, R.; Case, D. A.; Walker, R. C. An Overview of the Amber Biomolecular Simulation Package. *WIREs Comput. Mol. Sci.* **2013**, *3* (2), 198−210.
(76) Thompson, A. P.; Aktulga, H. M.; Berger, R.; Bolintineanu, D. S.; Brown, W. M.; Crozier, P. S.; In 'T Veld, P. J.; Kohlmeyer, A.; Moore, S. G.; Nguyen, T. D.; Shan, R.; Stevens, M. J.; Tranchida, J.; Trott, C.; Plimpton, S. J. LAMMPS - a Flexible Simulation Tool for Particle-Based Materials Modeling at the Atomic, Meso, and Continuum Scales. *Comput. Phys. Commun.* **2022**, *271*, 108171.
(77) Shirts, M. R.; Klein, C.; Swails, J. M.; Yin, J.; Gilson, M. K.; Mobley, D. L.; Case, D. A.; Zhong, E. D. Lessons Learned from Comparing Molecular Dynamics Engines on the SAMPL5 Dataset. *J. Comput. Aided Mol. Des.* **2017**, *31* (1), 147−161.
(78) Strader, M. L.; Feller, S. E. A Flexible All-Atom Model of Dimethyl Sulfoxide for Molecular Dynamics Simulations. *J. Phys. Chem. A* **2002**, *106* (6), 1074−1080.
(79) Gerlach, T.; Müller, S.; De Castilla, A. G.; Smirnova, I. An Open Source COSMO-RS Implementation and Parameterization Supporting the Efficient Implementation of Multiple Segment Descriptors. *Fluid Phase Equilib.* **2022**, *560*, 113472.
(80) Lin, S.-T.; Sandler, S. I. A Priori Phase Equilibrium Prediction from a Segment Contribution Solvation Model. *Ind. Eng. Chem. Res.* **2002**, *41* (5), 899−913.
(81) Baz, J.; Held, C.; Pleiss, J.; Hansen, N. Thermophysical Properties of Glyceline-Water Mixtures Investigated by Molecular Modelling. *Phys. Chem. Chem. Phys.* **2019**, *21* (12), 6467−6476.
(82) Sarman, S.; Wang, Y.-L.; Rohlmann, P.; Glavatskih, S.; Laaksonen, A. Rheology of Phosphonium Ionic Liquids: A Molecular Dynamics and Experimental Study. *Phys. Chem. Chem. Phys.* **2018**, *20* (15), 10193−10203.
(83) Müller-Plathe, F. Reversing the Perturbation in Nonequilibrium Molecular Dynamics: An Easy Way to Calculate the Shear Viscosity of Fluids. *Phys. Rev. E* **1999**, *59* (5), 4894−4898.
(84) Bhattad, A. Review on Viscosity Measurement: Devices, Methods and Models. *J. Therm. Anal. Calorim.* **2023**, *148* (14), 6527−6543.
(85) Kirkwood, J. G. Molecular Distribution in Liquids. *J. Chem. Phys.* **1939**, *7* (10), 919−925.
(86) Kirkwood, J. G.; Lewinson, V. A.; Alder, B. J. Radial Distribution Functions and the Equation of State of Fluids Composed of Molecules Interacting According to the Lennard-Jones Potential. *J. Chem. Phys.* **1952**, *20* (6), 929−938.
(87) Kusalik, P. G.; Laaksonen, A.; Svishchev, I. M. Spatial Structure in Molecular Liquids. In *Theoretical and Computational Chemistry*; Elsevier, 1999; Vol. 7, pp 61−97. DOI: 10.1016/S1380-7323(99)80036-3.
(88) Wang, Y.-L.; Sarman, S.; Kloo, L.; Antzutkin, O. N.; Glavatskih, S.; Laaksonen, A. Solvation Structures of Water in Trihexyltetradecylphosphonium-Orthoborate Ionic Liquids. *J. Chem. Phys.* **2016**, *145* (6), 064507.
(89) Lyubartsev, A. P.; Laaksonen, A. M. DynaMix - a Scalable Portable Parallel MD Simulation Package for Arbitrary Molecular Mixtures. *Comput. Phys. Commun.* **2000**, *128* (3), 565−589.
(90) Brehm, M.; Thomas, M.; Gehrke, S.; Kirchner, B. TRAVIS—A Free Analyzer for Trajectories from Molecular Simulation. *J. Chem. Phys.* **2020**, *152* (16), 164105.
(91) Frömbgen, T.; Blasius, J.; Dick, L.; Drysch, K.; Alizadeh, V.; Wylie, L.; Kirchner, B. Reducing Uncertainties in and Analysis of Ionic Liquid Trajectories. In *Comprehensive Computational Chemistry*; Elsevier, 2024; pp 692−722. DOI: 10.1016/B978-0-12-821978-2.00097-0.
(92) Humphrey, W.; Dalke, A.; Schulten, K. VMD - Visual Molecular Dynamics. *J. Mol. Graph.* **1996**, *14*, 33−38.
(93) Bergman, D. L.; Laaksonen, L.; Laaksonen, A. Visualization of Solvation Structures in Liquid Mixtures. *J. Mol. Graph. Model.* **1997**, *15* (5), 301−306.
(94) Dai, J.; Li, X.; Zhao, L.; Sun, H. Enthalpies of Mixing Predicted Using Molecular Dynamics Simulations and OPLS Force Field. *Fluid Phase Equilib.* **2010**, *289* (2), 156−165.
(95) Wu, X.; Liu, Z.; Huang, S.; Wang, W. Molecular Dynamics Simulation of Room-Temperature Ionic Liquid Mixture of [Bmim]-[BF4] and Acetonitrile by a Refined Force Field. *Phys. Chem. Chem. Phys.* **2005**, *7* (14), 2771.
(96) Monteiro, H.; Paiva, A.; Duarte, A. R. C.; Galamba, N. On the Not so Anomalous Water-Induced Structural Transformations of Choline Chloride-Urea (Reline) Deep Eutectic System. *Phys. Chem. Chem. Phys.* **2022**, *25* (1), 439−454.
(97) Nanavare, P.; Choudhury, A. R.; Sarkar, S.; Maity, A.; Chakrabarti, R. Structure and Orientation of Water and Choline Chloride Molecules around a Methane Hydrophobe: A Computer Simulation Study. *ChemPhysChem* **2022**, *23* (21), No. e202200446.
(98) Goltz, C.; Barbieri, J. B.; Cavalheiro, F. B.; Toci, A. T.; Farias, F. O.; Mafra, M. R. COSMO-SAC Model Approach for Deep Eutectic Solvent Selection to Extract Quercetin from Macela (A. Satureioides) and Experimental Process Optimization. *Biomass Convers. Biorefinery* **2023**, *13* (12), 11057−11066.
(99) Lu, T.; Chen, Q. Interaction Region Indicator: A Simple Real Space Function Clearly Revealing Both Chemical Bonds and Weak Interactions**. *Chemistry-Methods* **2021**, *1* (5), 231−239.
(100) Ma, C.; Guo, Y.; Li, D.; Zong, J.; Ji, X.; Liu, C.; Lu, X. Molar Enthalpy of Mixing for Choline Chloride/Urea Deep Eutectic Solvent + Water System. *J. Chem. Eng. Data* **2016**, *61* (12), 4172−4177.
(101) Ma, C.; Guo, Y.; Li, D.; Zong, J.; Ji, X.; Liu, C. Molar Enthalpy of Mixing and Refractive Indices of Choline Chloride-Based Deep Eutectic Solvents with Water. *J. Chem. Thermodyn.* **2017**, *105*, 30−36.
(102) Li, F.; Mocci, F.; Zhang, X.; Ji, X.; Laaksonen, A. Ionic Liquids for CO2 Electrochemical Reduction. *Chin. J. Chem. Eng.* **2021**, *31*, 75−93.
(103) Zafarani-Moattar, M. T.; Shekaari, H.; Sadrmousavi Dizaj, A. Investigation of Solute-Solvent Interactions in Binary and Quaternary Solutions Containing Lithium Perchlorate, Propylene Carbonate, and the Deep Eutectic Solvent (Choline Chloride/Ethylene Glycol) at T = (288.15 to 318.15) K. *J. Mol. Liq.* **2020**, *319*, 114090.
(104) Naik, P. K.; Mohan, M.; Banerjee, T.; Paul, S.; Goud, V. V. Molecular Dynamic Simulations for the Extraction of Quinoline from Heptane in the Presence of a Low-Cost Phosphonium-Based Deep Eutectic Solvent. *J. Phys. Chem. B* **2018**, *122* (14), 4006−4015.
(105) Lu, T. *Molclus Program*, 2023. http://www.keinsci.com/research/molclus.html.
(106) Bader, R. F. W. *Atoms in Molecules: A Quantum Theory*; Clarendon Press: Oxford, 1994.
(107) Busato, M.; Di Lisio, V.; Del Giudice, A.; Tomai, P.; Migliorati, V.; Galantini, L.; Gentili, A.; Martinelli, A.; D'Angelo, P. Transition from Molecular- to Nano-Scale Segregation in a Deep Eutectic Solvent - Water Mixture. *J. Mol. Liq.* **2021**, *331*, 115747.
(108) Busato, M.; Migliorati, V.; Del Giudice, A.; Di Lisio, V.; Tomai, P.; Gentili, A.; D'Angelo, P. Anatomy of a Deep Eutectic Solvent: Structural Properties of Choline Chloride: Sesamol 1:3 Compared to Reline. *Phys. Chem. Chem. Phys.* **2021**, *23* (20), 11746−11754.
(109) Mullins, E.; Oldland, R.; Liu, Y. A.; Wang, S.; Sandler, S. I.; Chen, C.-C.; Zwolak, M.; Seavey, K. C. Sigma-Profile Database for Using COSMO-Based Thermodynamic Methods. *Ind. Eng. Chem. Res.* **2006**, *45* (12), 4389−4415.